

IDENTIFICATION OF AUTONOMOUS SERVICE VEHICLE REQUIREMENTS

**Final Report
June 2016**

Principal Investigator

Eric Coyle
Assistant Professor of Mechanical Engineering

Co-Principal Investigator

Patrick Currier
Assistant Professor of Mechanical Engineering

Co-Principal Investigator

Brian Butka
Associate Professor of Computer and Electrical Engineering

Co-Principal Investigator

David Spitzer
ERAU Motorsports Director

Sponsored by the Florida Department of Transportation
(Contract #: BDV22-934-01)

Embry-Riddle Aeronautical University
600 S. Clyde Morris Blvd.
Daytona Beach, FL 32114-3900

DISCLAIMER PAGE

“The opinions, findings, and conclusions expressed in this publication are those of the authors and not necessarily those of the State of Florida Department of Transportation.”

METRIC CONVERSION CHART

SYMBOL	WHEN YOU KNOW	MULTIPLY BY	TO FIND	SYMBOL
LENGTH				
mm	millimeters	0.039	inches	in
m	meters	3.28	feet	ft
m	meters	1.09	yards	yd
km	kilometers	0.621	miles	mi

SYMBOL	WHEN YOU KNOW	MULTIPLY BY	TO FIND	SYMBOL
AREA				
mm ²	square millimeters	0.0016	square inches	in ²
m ²	square meters	10.764	square feet	ft ²
m ²	square meters	1.195	square yards	yd ²
ha	hectares	2.47	acres	ac
km ²	square kilometers	0.386	square miles	mi ²

SYMBOL	WHEN YOU KNOW	MULTIPLY BY	TO FIND	SYMBOL
VOLUME				
mL	milliliters	0.034	fluid ounces	fl oz
L	liters	0.264	gallons	gal
m ³	cubic meters	35.314	cubic feet	ft ³
m ³	cubic meters	1.307	cubic yards	yd ³

SYMBOL	WHEN YOU KNOW	MULTIPLY BY	TO FIND	SYMBOL
MASS				
g	grams	0.035	ounces	oz
kg	kilograms	2.202	pounds	lb
Mg (or "t")	megagrams (or "metric ton")	1.103	short tons (2000 lb)	T

SYMBOL	WHEN YOU KNOW	MULTIPLY BY	TO FIND	SYMBOL
TEMPERATURE (exact degrees)				
°C	Celsius	1.8C+32	Fahrenheit	°F

SYMBOL	WHEN YOU KNOW	MULTIPLY BY	TO FIND	SYMBOL
ILLUMINATION				
lx	lux	0.0929	foot-candles	fc
cd/m ²	candela/m ²	0.2919	foot-Lamberts	fl

SYMBOL	WHEN YOU KNOW	MULTIPLY BY	TO FIND	SYMBOL
FORCE and PRESSURE or STRESS				
N	newtons	0.225	poundforce	lbf
kPa	kilopascals	0.145	poundforce per square inch	lbf/in ²

Technical Report Documentation Page

1. Report No.	2. Government Accession No.	3. Recipient's Catalog No.	
4. Title and Subtitle Identification of Autonomous Service Vehicle Requirements		5. Report Date June 2016	
		6. Performing Organization Code	
7. Author(s) Eric Coyle, Patrick Currier, Brian Butka, David Spitzer		8. Performing Organization Report No.	
9. Performing Organization Name and Address Embry-Riddle Aeronautical University 600 S. Clyde Morris Blvd. Daytona Beach, FL 32114-3900		10. Work Unit No. (TRAVIS)	
		11. Contract or Grant No. BDV22-934-01	
12. Sponsoring Agency Name and Address Florida Department of Transportation 605 Suwannee Street, MS 30 Tallahassee, FL 32399		13. Type of Report and Period Covered Final Report May 2015-June 2016	
		14. Sponsoring Agency Code	
15. Supplementary Notes			
16. Abstract An expanding transportation infrastructure has increased the need for efficient methods of inspection and maintenance of this infrastructure. One solution to this problem is to use unmanned and autonomous systems for completing these service tasks. However, the sensing requirements of such systems have yet to be determined. To this end, the research team selected representative sensors from each of the primary sensing modalities expected on autonomous service vehicles (multi-beam LIDAR, automotive RADAR, GPS/INS system, and visible light camera) and mounted them on a commercial vehicle. Time-synchronized data was then collected in environments including urban areas, construction zones, interstates, and increased RF regions to evaluate the validity of the sensor data. Data was also collected to cover a range of weather conditions. Both manual and automated post-processing methods were used to determine the minimum data fidelity and other sensing requirements of an autonomous service vehicle completing the primary tasks of interest: roadside mowing and pavement inspection. This analysis resulted in a set of cases for which recommendations of requirements are made along with supporting evidence.			
17. Key Word Unmanned, Autonomy, Pavement Inspection, Roadside Mowing, LIDAR, RADAR, GPS		18. Distribution Statement No restrictions.	
19. Security Classif. (of this report) Unclassified.	20. Security Classif. (of this page) Unclassified.	21. No. of Pages	22. Price

Acknowledgments

The authors would like to thank the Florida Department of Transportation (FDOT) for supporting this research and promoting the use of autonomous technology within the state of Florida. The research team would specifically like to thank those involved in the Florida Autonomous Vehicles Initiative for their close involvement and the personnel of FDOT District 5 for providing a maintenance schedule which aided in collecting the data of interest. The authors would also like to thank GrayMatter Inc. for loaning the use of the Plan B vehicle and its sensors, which were used to complete this study.

Executive Summary

Autonomous vehicle studies typically focus on development of technologies and policies for operating vehicles that transport people and commodities on roadways. However, the use of autonomous vehicles for pavement and roadside management services, called *autonomous service vehicles*, have the potential to improve safety of these operations, provide financial benefit, and ensure they are completed reliably and efficiently. For instance, consider that the state of Florida spends over \$33.5 million annually on roadside management and that the state of Florida already has the second highest number of road construction and maintenance worker fatalities. This study primarily focuses on two of the most common service tasks, roadside mowing and pavement inspection. While the benefits of autonomous service vehicles are clear, current research fails to present acceptable sensing requirements for fielding systems to complete these tasks. This study addresses these shortcomings.

The study began by selecting representative sensors from each of the primary sensing modalities expected on autonomous service vehicles (multi-beam LIDAR, automotive RADAR, GPS/INS system, and visible light camera) and mounted them on a Ford Escape hybrid that was capable of autonomous operation (but would not be used autonomously in this study). Once mounted on the vehicle, data was collected in a variety of environments where autonomous service vehicles would operate, such as urban areas, construction zones, and interstates. These collections also took place over a range of weather conditions, including dusk, night, and rainy weather.

The data is synchronized and post-processed through a playback environment the team built using National Instruments LabVIEW, Google Earth and VeloView software packages. Using the playback environment, the team found data anomalies and characterized performance of these sensors in the environments under consideration. The research team also wrote automated search algorithms to search for GPS inaccuracies, the ability to detect line reflectivity and distinguish cut and uncut grass. In addition to the data analysis, a risk assessment was conducted in order to determine how standards should be set for communication with these autonomous systems.

The research team presents recommendations to ensure proper operation of autonomous service vehicles conducting roadside mowing or pavement inspection based on twelve use cases. These recommendations include to avoid the use of radar when passing under bridges, to avoid conducting pavement inspections in the rain and to use sensor fusion to mitigate GPS error. Each of the recommendations are supported with empirical evidence recorded using the sensor payload. Simple autonomy algorithms also found that LIDAR sensors may be effective at inspecting line reflectivity and determining areas with cut and uncut grass. This study also recommends bandwidth specifications for radio links based on modes of operation for pavement inspection and roadside mowing operations.

TABLE OF CONTENTS

DISCLAIMER PAGE.....	2
METRIC CONVERSION CHART	3
ACKNOWLEDGMENTS	5
EXECUTIVE SUMMARY	6
CHAPTER 1: INTRODUCTION	13
CHAPTER 2: VEHICLE MOUNTED PAYLOAD.....	14
Sensor Selection and Integration	14
Data Logging Software	17
CHAPTER 3: DATA COLLECTION	21
Data Collection Results.....	21
Examples of Collected Data.....	22
CHAPTER 4: ANALYSIS METHODS	27
Playback Environment	27
GPS Precision Algorithm.....	27
Line Detection Algorithm	28
Cut Grass Analysis.....	28
Communication System Risk Analysis.....	30
CISPR 25 and CISPR 12.....	31
Standards and Safety.....	32
CHAPTER 5: RECOMMENDATIONS.....	34
Mowing Risk Cases	34
Case 1: GPS accuracy in open areas	34
Case 2: Areas with heavy tree cover and tall buildings degrade even corrected GPS quality	34
Case 3: Resolution of LIDAR measurement needed to detect grass quality	36
Case 4: Rough ground will cause high vibrations and potentially cause data dropouts.....	37
Case 5: Effectiveness of LIDAR at recognizing construction objects.....	38
Case 6: Operating near cliffs or areas with large drop-offs	40
Case 7: Detection of obstructions and obstacles.....	41
Case 8: Mowing at night and in low-light scenarios.....	44
Mowing Operation Scenarios	45
Scenario: Line of Sight Operation	45
Scenario: Command Center Operation	45
Command Center Monitoring.....	45
Pavement Inspection Risk Cases	46
Case 1: Detection of road lines and characterizing line reflectivity	46
Case 2: Detection of potholes	47
Case 3: The effect of wet roads on pavement inspection and autonomous operation	49

Case 4: Operating under bridges	50
Pavement Inspection Operation Scenarios.....	52
Scenario: Manned Data Recording	52
Scenario: Automated Data Recording	52
Scenario: Control Center Monitoring	53
CHAPTER 6: CONCLUSIONS	54
REFERENCES	55

LIST OF FIGURES

Figure 1: Plan B vehicle used for data collection. Mounting locations of the Velodyne LIDAR, Continental Radar, GPS antennas, and camera are as indicated.	15
Figure 2: Velodyne HDL-64E LIDAR (left) and OXTS RT3000 Series GPS and Inertial System (right) selected as part of the vehicle mounted payload.	15
Figure 3: The Continental ARS 308-2C automotive radar (left) and Samsung SNO-7084R camera system (right) selected as part of the vehicle mounted payload.	16
Figure 4: Samsung Camera and Continental Radar as mounted on the Plan B vehicle.	16
Figure 5: A snapshot of the first 20 targets reported by the ARS 308-2C radar. These measurements are extracted from the raw data bytes transmitted via CAN protocols.	18
Figure 6: Verification plot of objects identified by the radar system (top). The highlighted green box contains the object location of the green Honda Accord less than 5 meters from the radar, the red box shows the location of the red Ford Explorer 20 meters from the radar, and the Blue box shows the object points corresponding to the fence line at over 100 meters from the radar. The lower image is a camera image taken when placed in the mounting location of the radar on the Plan B vehicle.	19
Figure 7: Snapshot view of the primary control module for data recording and monitoring sensor status during data collections.	20
Figure 8: Snapshot of data recorded on I-95 during rainy weather. Radar returns are plotted in the upper left position, camera image in the top right position, LIDAR returns plotted in the bottom left position, and GPS location show in the bottom right position.	23
Figure 9: Snapshot of data recorded on dirt and gravel roadways in Volusia County.	24
Figure 10: Snapshot of data recorded on local roadways the evening after roadside mowing has been completed.	25
Figure 11: Snapshot of data recorded in downtown Orlando, FL around tall buildings.	26
Figure 12: Camera view of grass detection environment	29
Figure 13: Unprocessed LIDAR returns of grass environment	29
Figure 14: Unprocessed single-laser LIDAR returns.	30
Figure 15: A sample of the LASER ring in the previous figure LIDAR points classified as road (blue) and grass (green)	30
Figure 16: Tree Cover on Old Dixie Highway in Ormond Beach, FL.	35
Figure 17: A snapshot of the GPS path during traversal on Old Dixie Highway in Ormond Beach, FL.	35
Figure 18: Sample result of Asphalt (blue), Cut Grass (green) and Uncut Grass (yellow) detection.	36
Figure 19: Samples of measured vertical acceleration of the vehicle on a dirt road (left) and on a paved roadway (right).	37
Figure 20: Data loss shown in the LIDAR playback	38
Figure 21: Camera view of construction zone, including concrete barriers and construction barrels.	39
Figure 22: LIDAR returns in a construction zone. High reflectivity objects make more apparent markers of construction areas.	39
Figure 23: Camera Image when crossing over a bridge.	40
Figure 24: LIDAR data recorded when crossing over a bridge.	40
Figure 25: Vehicle obstruction as viewed by the camera and LIDAR. The man working on the	

truck is highlighted with a red circle in the camera image and LIDAR plot. The area where the man is working is highlighted with a red circle on the radar plot. The two green dots above the red circle in the radar plot are from the truck and trailer.	42
Figure 26: Plastic mowing obstruction as viewed by the camera, LIDAR and radar.....	43
Figure 27: LIDAR data collected during daytime (top) and at night (bottom) on the roadway. ...	44
Figure 28: Line Detection results for Tomoka Farms Rd, in Port Orange, FL. The lines here show the detected color of the road line as viewed by the onboard camera and the horizontal position within the camera frame.....	46
Figure 29: Sample pothole data on local roadways in Volusia County.....	48
Figure 30: Camera and LIDAR view of road lines in rainy conditions. There is no standing water on the roadway.....	49
Figure 31: LIDAR view of a road covered in a thin layer of water (less than 1 cm) due to heavy rain	50
Figure 32: Pedestrian walkway as viewed by the camera and RADAR.....	51
Figure 33: LIDAR view of the pedestrian walkway scene. The walkway is not visible since the LIDAR beams point up at a maximum of 2 degrees with respect to the horizontal plane.....	52

LIST OF TABLES

Table 1: The approved list of test conditions which include operating environments and weather conditions.....	21
Table 2: Summary of Collected Data.....	21
Table 3: CISPR and ISO Standards applicable to Autonomous Service Vehicles	31
Table 4: Example of Test Severity Levels for Incident Field	33
Table 5: Example of Frequency Bands	33
Table 6: Example of Field of View Severity Levels Matched to Frequency Bands.....	33
Table 7: Summary of LIDAR intensity analysis for line reflectivity	47

LIST OF ACRONYMS

LIDAR – Light Detection and Ranging

GPS – Global Positioning System

RMS – Root Mean Squared

ISO – International Standard Organization

CISPR – Comité International Spécial des Perturbations Radioélectriques (in English: International Special Committee on Radio Interference)

FPSC – Functional Performance Status Classification

RF – Radio Frequency

Chapter 1: Introduction

Effective July 1, 2012, the Florida Legislature authorized the testing of autonomous vehicles in Florida [1]. Since the inception of this law, the state of Florida has established a leadership position in the development of autonomous vehicles and related technologies. The primary focus of autonomous vehicle studies has been related to the development of technologies and policies for operating vehicles that transport people and commodities on roadways. However, the use of autonomous vehicles for pavement and roadside management services, herein referred to as autonomous service vehicles, have the potential to improve safety of these operations, ensure they are completed reliably, completed efficiently, and provide financial benefit. Candidate services to be conducted by autonomous service vehicles include roadside mowing and pavement inspection.

The state of Florida spends over \$33.5 million annually on roadside management, with over 25 percent of that being mowing costs [2]. Furthermore, Governor Rick Scott has proposed the use of over \$242 million for maintenance and repair of Florida roadways as part of his ‘Keep Florida Working’ budget. This initiative has the potential to improve local economies by employing more workers, but these workers are at risk of being struck by a construction or motor vehicle. In fact, the state of Florida already has the second highest number of road construction and maintenance worker fatalities [3]. The use of autonomous service vehicles can significantly improve occupational safety by moving workers farther from moving vehicles.

In addition to public roadways, airports must complete a substantial number of service tasks. The state of Florida has 129 public, private and military airports [2]. Mowing at airports, which is required by Federal Aviation Regulations Part 139, attracts birds due to uncovered seeds and insects. An estimated 11,000 bird strikes occur each year resulting in a \$1.2 billion loss. While human operators must mow during the day, an autonomous service vehicle may be able to operate at night when fewer flight operations occur, reducing the likelihood of bird strikes. These autonomous vehicles may also be able to operate in extreme weather conditions, which may further reduce the risk of personal injury.

While the benefits of autonomous service vehicles are clear, current research fails to present acceptable sensing requirements for fielding systems to complete these tasks. The lack of requirements is largely due to the development of algorithms and the collection of data in laboratory or highly-controlled environments instead of the operating environment of such platforms. This project develops sensing requirements for autonomous service vehicles by data collection from the operating environments and subsequent data analysis. Generating these requirements is a precursor to the use of autonomous service vehicles on and in proximity to public roadways.

Chapter 2: Vehicle Mounted Payload

The first step in determining sensing requirements was to identify the primary sensing modalities needed to field autonomous service vehicles. For this purpose, the research team focused on the two primary service tasks of roadside mowing and pavement inspection (line striping and pavement integrity). Completing these tasks require sensors for both autonomous navigation and identification of vehicle surroundings (terrain, obstacles, grass status and pavement integrity).

The primary sensors used in autonomous ground vehicle navigation are GPS, Inertial Measurement Units, and a Magnetic Compass. These sensors enable an autonomous vehicle to determine the vehicle state of linear and angular position and velocity. For perception purposes, visible light cameras, LIDAR and radar are the most common sensors used by autonomous ground vehicles. For both navigation and perception sensors, the team sought to select off-the-shelf products with high data fidelity (accuracy and resolution). Through the use of high-end equipment, the data can be degraded in post-processing to find the lower limit of sensor specifications suitable to perform the service vehicle tasks autonomously.

Sensor Selection and Integration

The research team first selected a research platform to conduct the study. The Plan B vehicle, shown in Figure 1, was selected for this purpose. Plan B is an autonomous Ford Escape on loan to Embry-Riddle Aeronautical University (ERAU) from its developers at GrayMatter Inc. and originally developed to compete in the DARPA Grand Challenge. This platform has an Ethernet communication backbone for communication with the vehicle sensors and the autonomous software system. While this project did not utilize the autonomous software systems, the team chose to utilize Ethernet communications, where possible, due to the reliability and high throughput of this protocol. As an electric hybrid, this vehicle is capable of producing significantly more electrical power than a typical gasoline powered vehicle, which typically have low power 12V direct current electrical power onboard. Plan B is also modified with 120V alternating current power through a high power inverter. This enabled the research team to select sensors with a wide array of power options, with minimal changes to the vehicle. Thus the built-in communication infrastructure and power systems made the Plan B vehicle a logical and effective choice for this project.

After vehicle selection, the team proceeded to select and acquire the sensing and computing systems for the vehicle mounted payload. As part of the loan agreement with GrayMatter Inc., the research team had access to a Velodyne HDL-64E LIDAR and OXTS RT3000 Series GPS/Inertial Measurement system, which were selected for use in this study. The OXTS RT3000 Series GPS (Figure 1) has a variety of high end features that include inertial corrections to GPS, dual antennas and a 100Hz update rate. Measurements from this system are highly accurate with reported accuracies up to 2cm for position, 0.1 km/h for velocity, 0.1° for heading and 0.05° for pitch and roll accuracy.

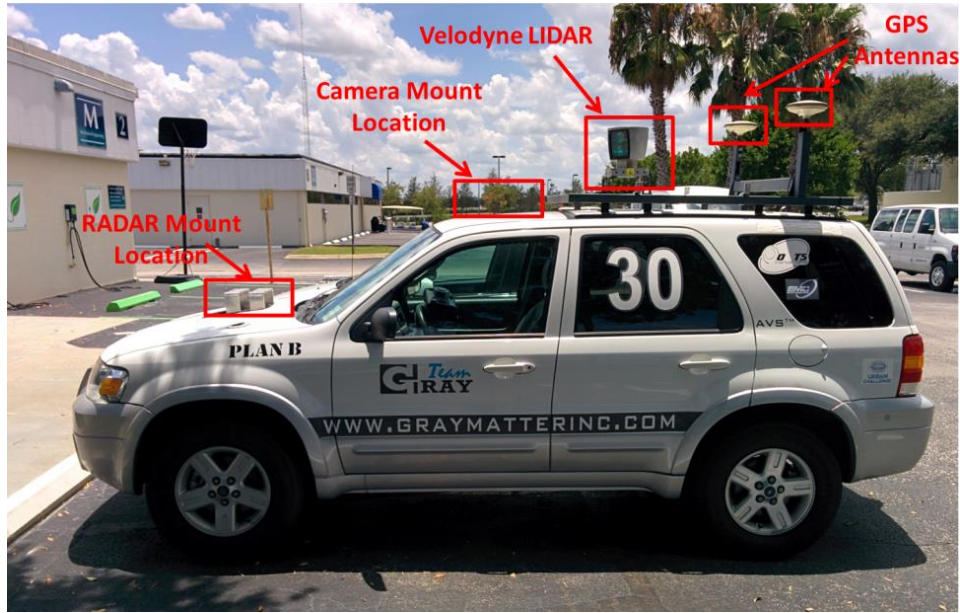


Figure 1: Plan B vehicle used for data collection. Mounting locations of the Velodyne LIDAR, Continental Radar, GPS antennas, and camera are as indicated.

The Velodyne HDL-64E (Figure 2) is a 64 laser beam ranging sensor that provides up to 2.2 million data points per second at update rates of 5-15Hz, with a 26.8° degree vertical FOV and 360° horizontal field of view. Range estimates can be provided by this sensor at distances up to 50m for low reflectivity objects (less than 0.1 reflectivity) and up to 120m for high reflectivity objects (greater than 0.8 reflectivity). This sensor provides one of the highest point densities currently available in commercial LIDAR systems, making it a perfect simulator for lower capability sensors by ignoring specific lasers and subsampling for lower angular resolutions.

The Velodyne and GPS sensors were mounted on the Plan B vehicle as indicated in Figure 1. These mounting locations are typical of an autonomous service vehicle, which would mount GPS antennas at the highest point of the vehicle and LIDAR sensors in locations that maximize visibility.



Figure 2: Velodyne HDL-64E LIDAR (left) and OXTS RT3000 Series GPS and Inertial System (right) selected as part of the vehicle mounted payload.

As part of the vehicle mounted payload, the team sought to incorporate a commercial radar solution for object detection and velocity estimation, which are needed to detect possible collisions. While important for roadside mowing and pavement inspection, the team expects FDOT attenuator trucks are more likely to benefit from this capability. The research team did not own any compatible radar solutions and therefore investigated off-the-shelf solutions. The team found that there are two primary automotive radar manufacturers, Continental and Delphi. Upon reviewing the available products, the Continental ARS 308-2C automotive radar (see Figure 3) was selected over the Delphi systems because it provided access to additional low-level data, such as radar cross section and error estimates. While automotive radar are traditionally mounted on the front bumper, for this project the radar was mounted above the hood and directly below the alternative mounting location for the Velodyne HDL64E, as shown in Figure 4. This mounting location did not require modifying any of the structural components of the vehicle, which was on loan to the University. The team did not find any negative effects from mounting the radar in close proximity to the reflective hood. This is likely due to the limited vertical field of view of this sensor or the shallow angle reflections would make with the hood, preventing them from returning to the radar to be interpreted.



Figure 3: The Continental ARS 308-2C automotive radar (left) and Samsung SNO-7084R camera system (right) selected as part of the vehicle mounted payload.



Figure 4: Samsung Camera and Continental Radar as mounted on the Plan B vehicle.

A visible light camera was also included in the vehicle payload for verifying the presence of objects from the LIDAR and radar and to investigate the appearance of faded road lines during pavement inspection. While ERAU owns many vision solutions, the research team determined the camera solution needed to have a horizontal field of view wider than the radar (56 degrees) and must withstand a variety of environmental factors, including rain, heat and fog. As none of the ERAU owned assets met these requirements, designing enclosures, purchasing a new lens for a currently owned system, and the possible acquisition of a new camera system were considered.

Due to its rain and dust resistant rating and Ethernet communication protocol, the team selected the SNO-7084R Samsung Security Camera, as seen in Figure 4, which provides a maximum resolution of 3 megapixels and framerates up to 60 fps (the team recorded video at 1080p and 60 fps). The camera also has a motorized variable focal length, resulting in a field of view from 100.2° to 35.38°. Additional functionality includes audio recording, motion detection, and programmable control of the camera functions. The camera was mounted on the Plan B vehicle above the windshield using the existing railings that support mounting of the GPS and LIDAR (see Figure 4).

The team also investigated the use of a spectrum analyzer for inclusion in the vehicle mounted payload. The team found the most pertinent part of the spectrum to be the 400 MHz to 6 GHz range, as this includes the standard 434 MHz, 900MHz, 2.4GHz and 5.8GHz communication bands used in most autonomous systems, and covers the L1 1.6 GHz and L2 1.2GHz frequency bands of GPS signals. While software defined radio solutions are commercially available for lease or purchase that would enable measurement of these parts of the spectrum, the team looked at existing RF standards in the automotive industry before pursuing this option. This investigation found that there are three commonly referenced standards, ISO 11452, CISPR 25, and SAE J1113 [5], [6], [7]. Since rigorous standards already exist, data collected from a spectrum analyzer would be unlikely to contradict these standards. Thus, instead of collecting RF data as part of the vehicle payload, FDOT approved the team conducting a risk assessment to determine the appropriate level of compliance needed for autonomous service vehicle communications.

Data Logging Software

As part of the vehicle mounted payload, the researchers created software using the National Instruments LabVIEW environment to communicate with the payload devices and log the data coming from these devices. The GPS, LIDAR and camera systems all communicate via Ethernet protocols which are simultaneously routed to a logging computer via an Ethernet switch in the Plan B vehicle. The radar communicates via CAN protocols which are converted to Serial Data using a CAN to USB converter plugged directly into the data logging computer.

Within the software, there is a sensor module dedicated to communication with each device running in a parallel configuration for reduced lag and improved data synchronization. The radar and GPS modules take the raw data messages and extract the measurements based on the message format provided in the sensor datasheets. A snapshot of the extracted data from the radar is shown in Figure 5. The camera gave a JPEG compressed video stream which is saved directly to the data logging computer, as no further processing is required. The research team

originally wrote a module to extract raw LIDAR data, but the nearly 2.2 million data points each second this sensor can produce created lag in the system when viewing within LabVIEW. Thus, the LIDAR data is saved directly in its raw form to prevent delay and data synchronization errors.

Target Data													
Target	Dist_RMS	Ang_RMS	Vrel_RMS	Vrel	Dist	Prob	Length	Width	Ang_Stat	Type	Angle	Cross-Section	Near Targets
0	0	0	0	0	0	0	0	0	0	0	0	0	7
1	0	2	0.01	0.02	4.7	0	1.1	1	2	0	-16.7	-6.8	Far Targets
2	0	7	0.01	0.05	20.8	0	2.6	0	2	2	26.6	-3.5	12
3	0	1	0.01	0.44	25.3	0	1.5	1.7	2	1	0	7.9	
4	0	1	0.01	0.38	28.8	0	0.1	0	2	1	-1.6	-3.7	
5	0	3.5	0.01	0.2	38.8	0	0.2	0	2	2	-1.1	-4	
6	0	1	0.01	-0.16	44.1	0	0	5.4	2	0	1.5	0	
7	0	2	0.01	-0.16	47.5	0	0.6	0.8	2	1	22.2	-0.2	
8	0	1	0.01	0.47	44.3	0	0	0.2	2	1	-2.1	-0.4	
9	0	3.5	0.01	0.44	44.2	0	0	0	2	2	-1.1	1.2	
10	0	2.1	0.01	-0.19	48.5	0	0	0	2	1	20.2	-0.2	
11	0	1.1	0.01	-0.07	44	0	0	0	2	1	6	-0.4	
12	0	3.5	0.01	-0.16	46.5	0	0	0	2	2	20.5	-2.5	
13	0	2	0.01	-4.21	59.6	0	0	0	1	1	15.5	5.9	
14	0	1	0.01	-4.78	45.2	0	0	0	1	1	8.5	3.9	
15	0	2	0.01	-4.69	58.5	0	0.3	0.1	1	1	16.7	16.4	
16	0	3.5	0.01	-1.51	56.4	0	0	0	1	2	13.5	2.9	
17	0	0	0.01	-0.01	0	0	0	0	0	0	0	-40	
18	0	0	0.01	-0.01	0	0	0	0	0	0	0	-40	
19	0	0	0.01	-0.01	0	0	0	0	0	0	0	-40	
20	0	0	0.01	-0.01	0	0	0	0	0	0	0	-40	

Figure 5: A snapshot of the first 20 targets reported by the ARS 308-2C radar. These measurements are extracted from the raw data bytes transmitted via CAN protocols.

In addition to each sensor having its own communication module, a primary control module was written in LabVIEW to monitor the status of each sensor, select sensor data to log, and control recording functionality. A snapshot of this interface is shown in Figure 7. The interface also allows the team to add comments and notes to the data logs such as location and weather condition. The camera, GPS, and radar data can be viewed under adjoining tabs across the top of the interface. As the LIDAR data is saved and not extracted within LabVIEW, real-time viewing of this data must be done through the VeloView software provided by Velodyne. The data collection software was field tested on the ERAU campus to ensure data was being logged properly and the data was extracted from the raw messages accurately, as seen for the radar in Figure 6.

The use of GPS time stamps for data synchronization was considered, but only the LIDAR natively supported this functionality. Instead, all data is synchronized by referencing the internal clock on the data logging computer based on time of arrival of the data to the computer. This provides synchronization to within 10 msec, which is the fastest sampling rate of any of the payload sensors. The data logging computer uses a solid stated drive to store the data locally, which increases the speed at which data is written to the drive and prevents data corruption that

can occur when using hard drives in moving vehicles. The data is logged in the native LabVIEW format to further improve logging speed, but can be extracted in a post-processing step as discussed in Chapter 4.

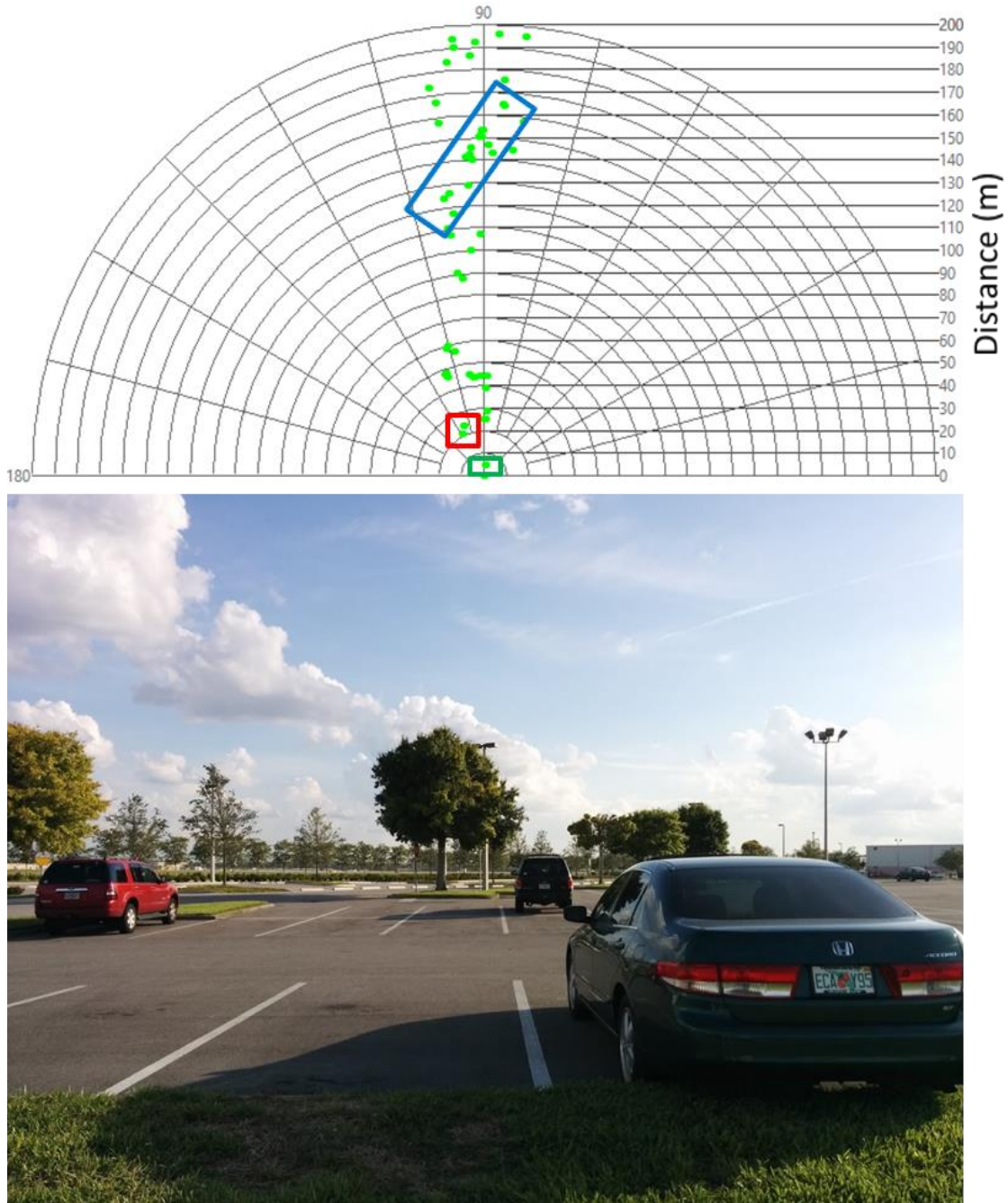


Figure 6: Verification plot of objects identified by the radar system (top). The highlighted green box contains the object location of the green Honda Accord less than 5 meters from the radar, the red box shows the location of the red Ford Explorer 20 meters from the radar, and the Blue box shows the object points corresponding to the fence line at over 100 meters from the radar. The lower image is a camera image taken when placed in the mounting location of the radar on the Plan B vehicle.

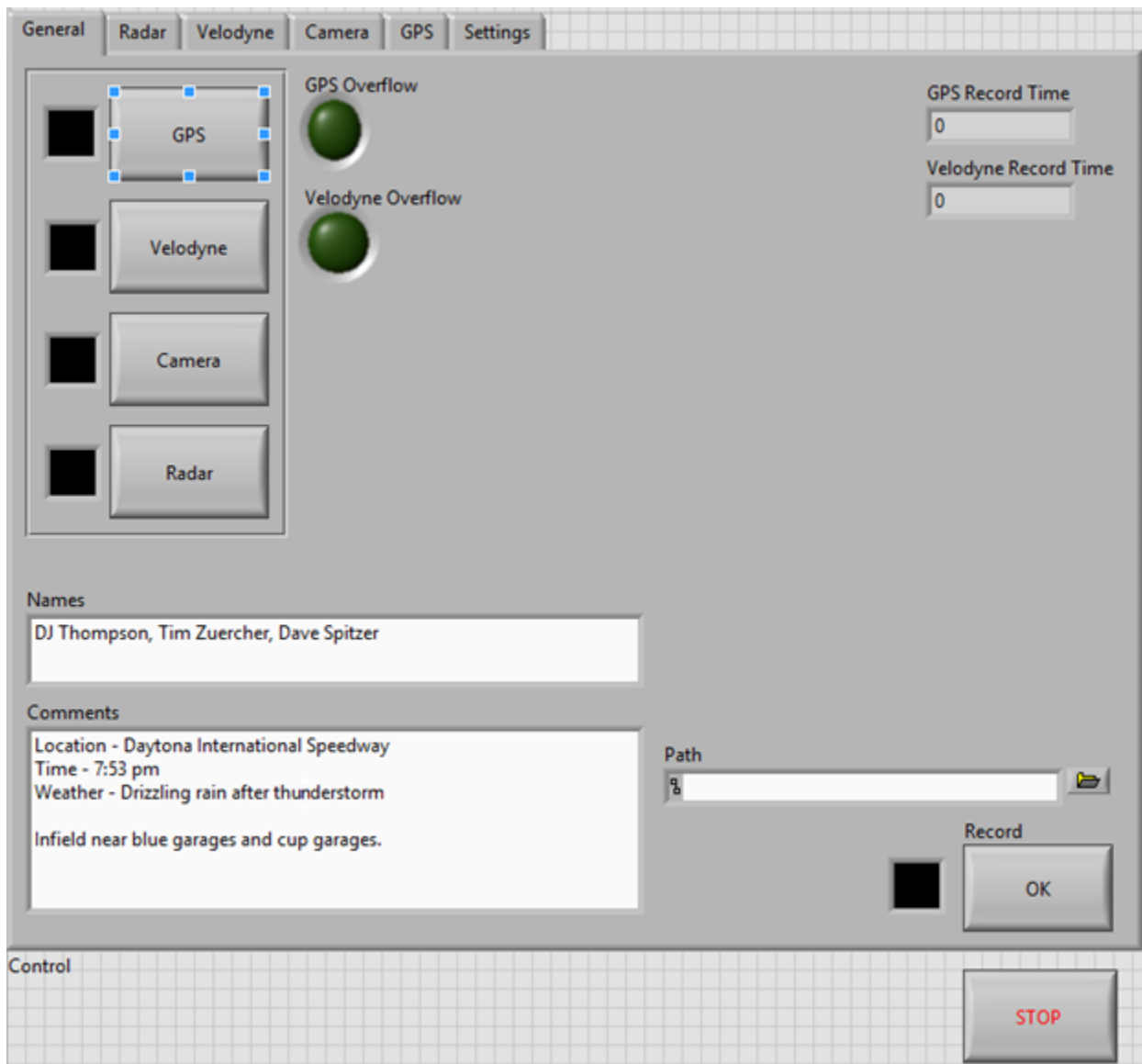


Figure 7: Snapshot view of the primary control module for data recording and monitoring sensor status during data collections.

Chapter 3: Data Collection

The project required collecting data from the vehicle mounted payload in a variety of environments and scenarios where an autonomous service vehicle will operate. The team began the data collection process by identifying a set of operating environments and weather conditions in which data should be collected. These cases ranged from normal operating conditions of service vehicles to the more severe environments that can occur due to weather, traffic and other hazards that may affect sensor performance. While compiling this list, the team primarily focused on the tasks of pavement inspection (e.g. striping) and roadside mowing, which were identified in the proposed scope of work as the primary service tasks of interest. The list was reviewed and approved by FDOT program managers through a teleconference and are shown in Table 1. The research team then sought to collect 5 or more data sets and 20 minutes of total data in each operating environment and weather condition. The team monitored the status of each sensor through the LabVIEW interface.

Table 1: The approved list of test conditions which include operating environments and weather conditions.

Operating Environments	Weather Conditions
Traffic Congestion	Rain
Tall Buildings	Night
High RF	Dusk or Dawn
Construction and Striping Areas	Sunny
Cut & Uncut Grass	Overcast
Heavy Vibrations	

Data Collection Results

Based on the previously approved list, the research team identified roadways within 150 miles of the ERAU campus that contained the desired operating environments. The research team also monitored the weather to ensure data collection across the desired set of weather conditions. The completed list of collected data is given below in Table 2 and organized by test location.

Table 2: Summary of Collected Data

Test Location	Condition(s) Collected	Collection Time	File Size
A1A (Bike Week)	Pedestrians, Bike Congestion	75 Minutes	31 GB
Daytona Beach International Airport	High RF, Air Traffic	45 Minutes	18 GB
Daytona International Speedway	High RF	25 Minutes	11.6 GB
Downtown Orlando	Tall Buildings, Traffic Congestion	20 Minutes	8.9 GB
I-4	Traffic Congestion, Construction, Sunny, Dusk, Night	140 Minutes	55.6 GB
I-95	Road Construction, Overpasses, Rain	130 Minutes	53.2 GB
Local Private Roadways	Day, Dirt/Gravel, Rough Terrain	45 Minutes	18 GB
Local Public Roadways	Sunny, Overcast, Night, Dusk, Rain, Cut & Uncut Grass	120 Minutes	49.5 GB
Stationary Testing	Day/Night, Sensor Testing	40 Minutes	15.8 GB
Total		640 Minutes	262 GB

In total, over ten hours and 262 GBs of data were collected by the research team. This complies with the stated goal of 20 minutes of data collected from each test condition. However, it should be noted that some test locations provided an opportunity to collect data under multiple test conditions at once. For instance, the research team was able to collect data at dusk, night and during heavy traffic on I-4 between Daytona Beach and Orlando. It should also be noted that the file sizes of these data collections were significantly less than the research team originally projected. This is because the camera did not natively provide uncompressed images, but instead had a compressed output. This compression was found to give an indistinguishable difference in image quality.

Examples of Collected Data

Figure 8 through Figure 11 show samples of the collected data in four different test locations. These figures display the location of radar returns in front of the vehicle (green dots in the upper polar plot), an image from the onboard camera (upper right), the LIDAR returns (lower left), and the location of the vehicle as reported on Google maps (lower right).

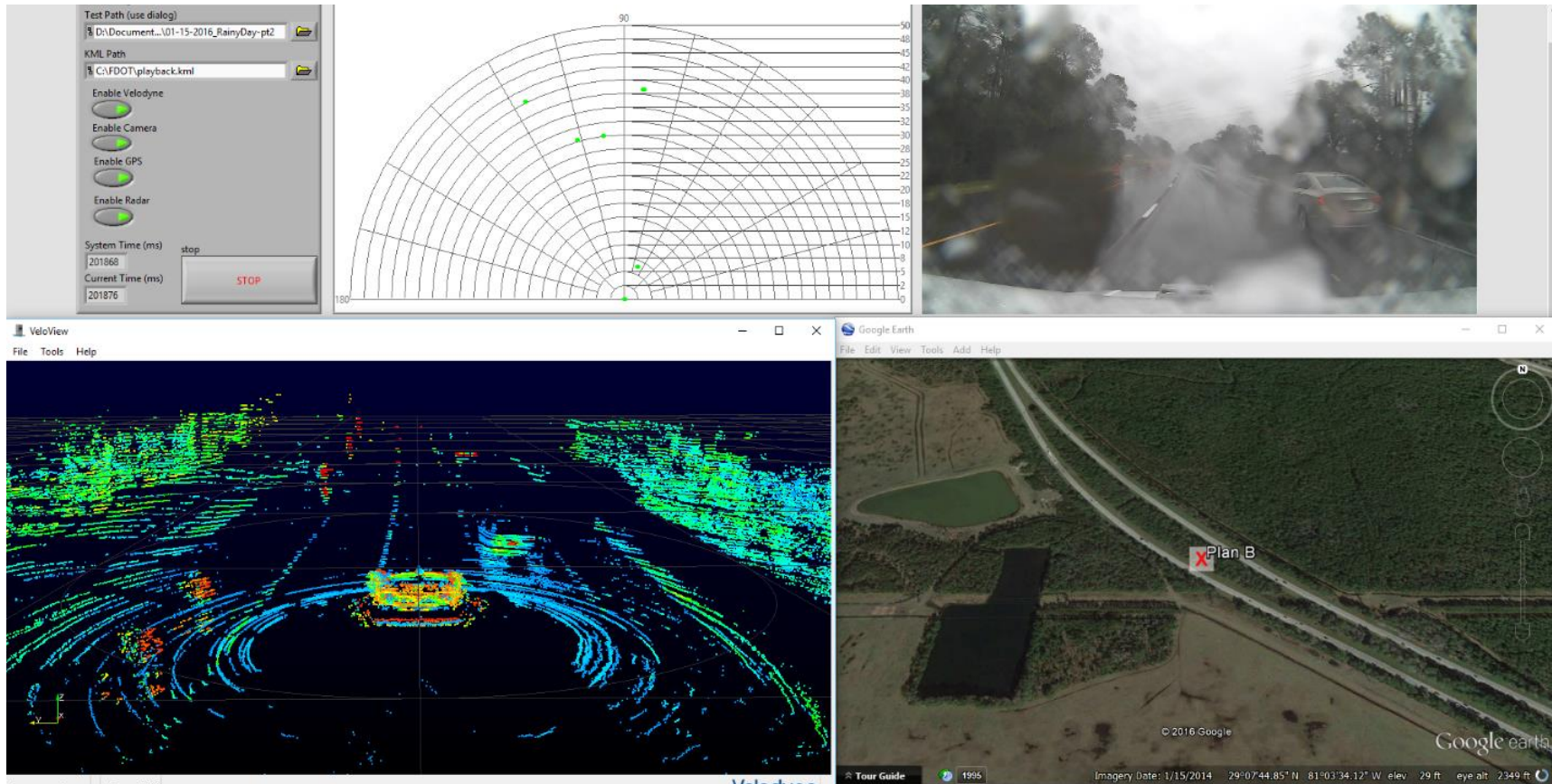


Figure 8: Snapshot of data recorded on I-95 during rainy weather. Radar returns are plotted in the upper left position, camera image in the top right position, LIDAR returns plotted in the bottom left position, and GPS location show in the bottom right position.

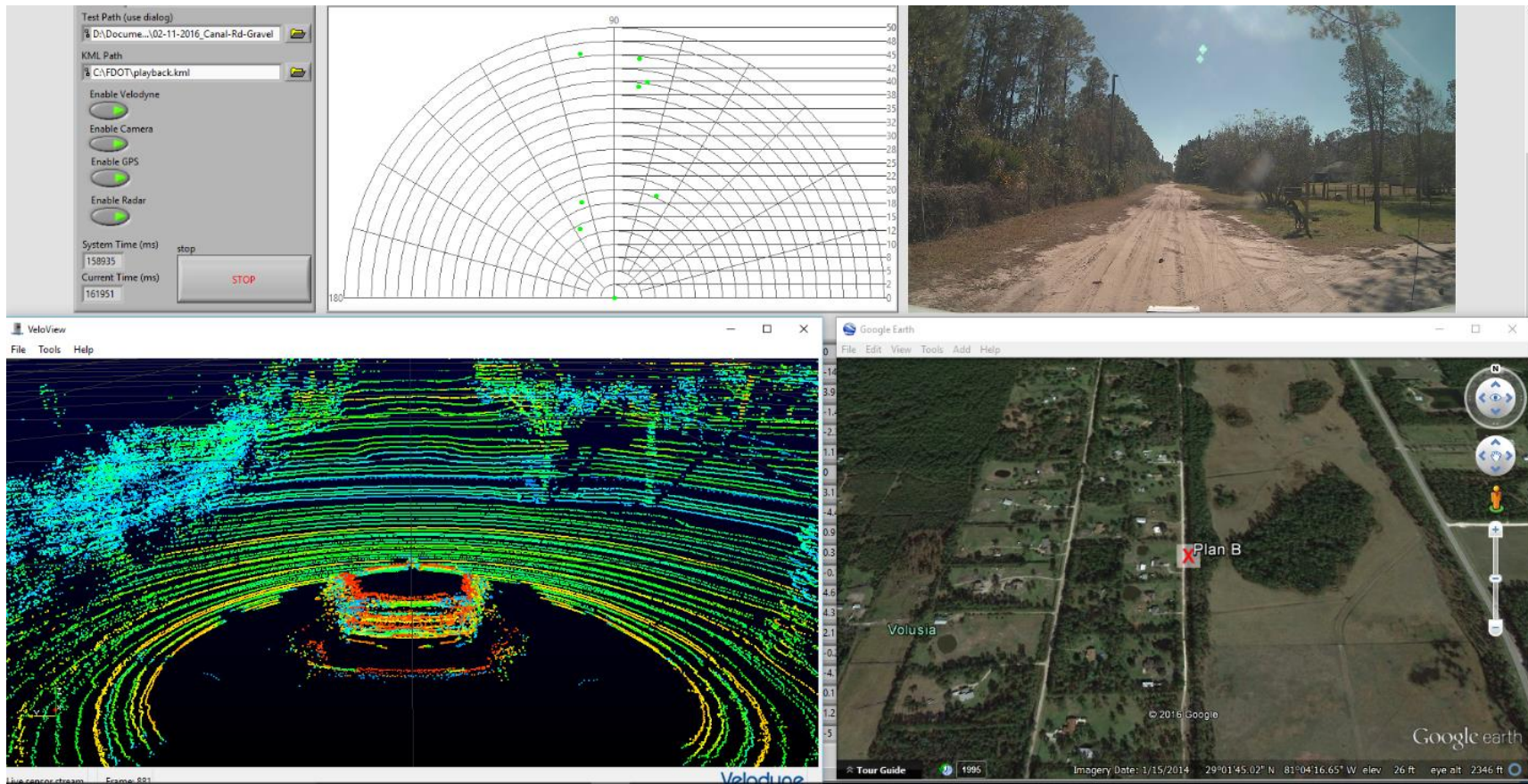


Figure 9: Snapshot of data recorded on dirt and gravel roadways in Volusia County.

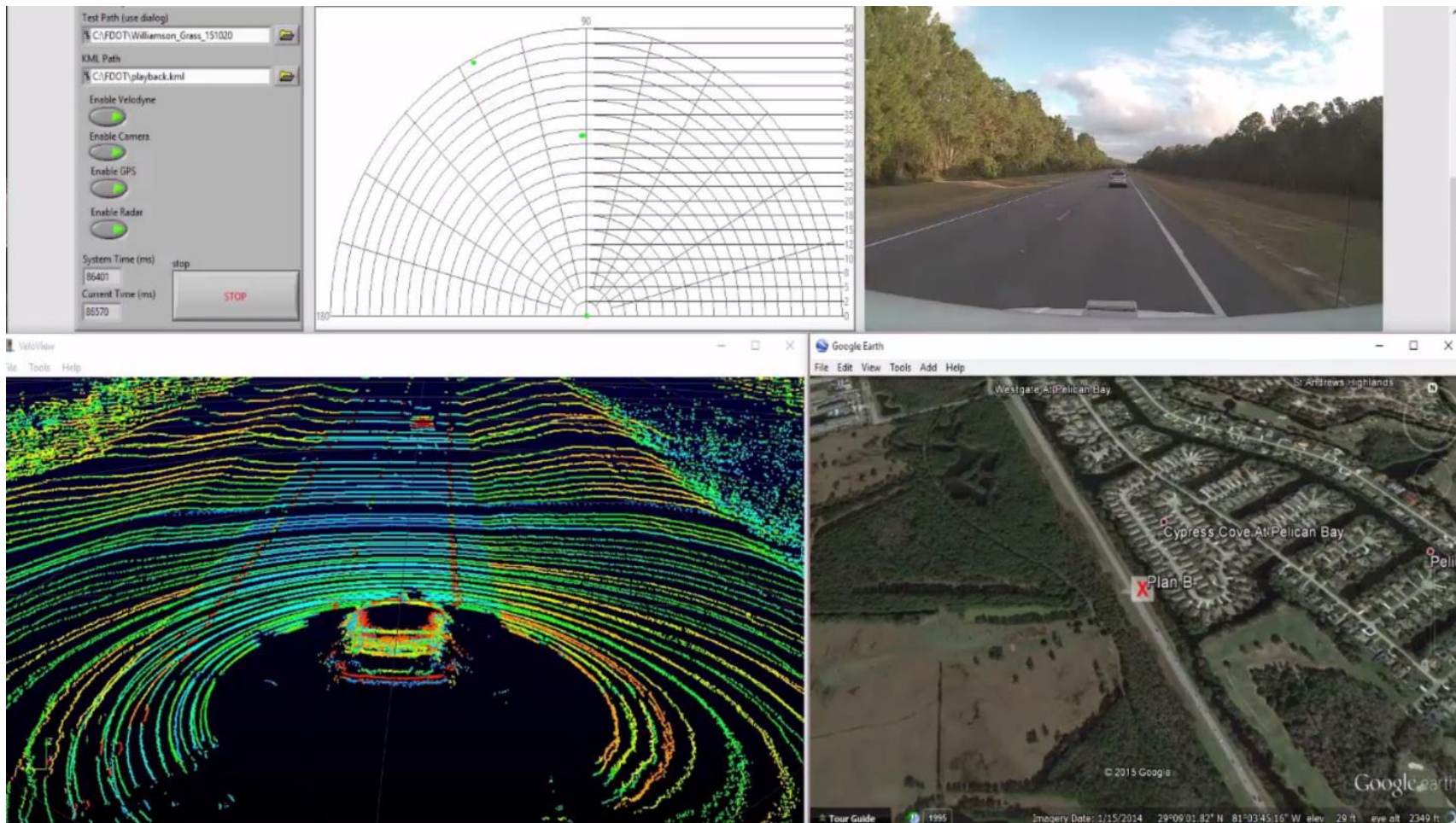


Figure 10: Snapshot of data recorded on local roadways the evening after roadside mowing has been completed.

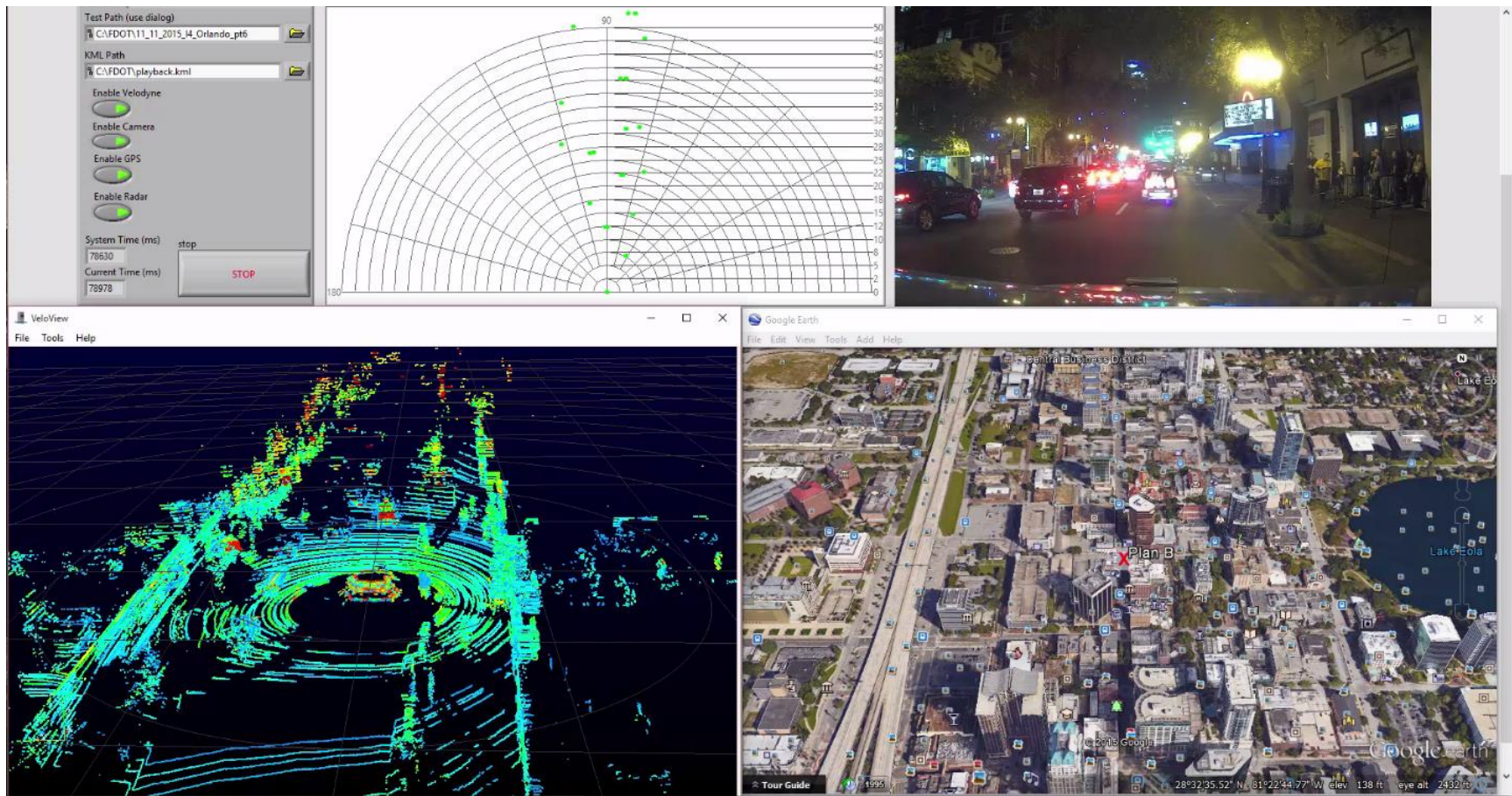


Figure 11: Snapshot of data recorded in downtown Orlando, FL around tall buildings.

Chapter 4: Analysis Methods

To analyze the collected data, the team pursued both manual and automated methods of data inspection. For manual inspection the team created a playback environment using LabVIEW, Google Earth and VeloView that plots and synchronously plays back the data recorded from the GPS, Radar, LIDAR, and camera. For the operating environments and weather conditions under consideration, viewing the data through this playback environment provided a qualitative measure of sensor performance, which was necessary to make recommendations for requirements. However, some aspects of autonomous vehicles conducting roadside mowing and pavement inspection were expected to require more accurate quantitative measures of performance. These key measures were determining GPS accuracy and dropout, the reflectivity of the road lines, and needs for distinguishing cut grass from other terrains. In each of these cases, the team wrote algorithms to conduct a basic analysis of the data and quantify required sensor performance. As previously discussed, the team also conducted a risk analysis to determine an appropriate level of compliance for radio frequency (RF) communications. The following subsections describe the playback environment, algorithm designs and background of the risk analysis.

Playback Environment

For the playback environment the team sought to display data from all the payload sensors in a time synchronized manner on a single display. To accomplish this, the team initially created separate plots for each sensor within LabVIEW. However, the result had significant lag due to plotting a high number of three dimensional points through the LabVIEW 3D plot tools. To address this, the team used LabVIEW to simulate the raw data coming from the Velodyne LIDAR, which was then streamed to the VeloView software provided by Velodyne LIDAR for visualization. Similarly, the team used LabVIEW to write GPS data to a file format that could be continuously read by Google Earth. This enabled the team to display a satellite view of the GPS location provided by Plan B. The radar and camera data were displayed in a LabVIEW window that could be viewed simultaneously with VeloView and Google Earth. The screenshots in Figure 8 through Figure 11 are sample results from this playback environment.

GPS Precision Algorithm

By default, many GPS systems will report estimated error. This error is typically computed by finding the error in location of a receiver in a known location or by computing the RMS error coming from each independent set of satellites the GPS is currently using. While this gives some measure of reliability, situations still occur where GPS sensors can output unusually large jumps in position without reporting a similarly high error estimate. Thus, GPS sensors natively estimate accuracy, but individual readings or readings over a short time period can exceed the reported accuracy. To address this, the team sought a mechanism to characterize the accuracy and precision of the GPS readings. The Oxford system used in this study uses sensor fusion to combine estimates from the inertial measurement unit and GPS for the purpose of providing a more accurate measurement of GPS location and velocity (which are part of the vehicle state).

Thus, the accuracy of the system used in this study is analogous to that of other high-end GPS/INS systems that perform sensor fusion. By comparison, a 2013 survey of sensing technologies for construction applications stated that basic and differential GPS units can be expected to provide an accuracy of 1-10m, while a GPS/INS system can obtain accuracy levels of less than 5cm [8].

To estimate GPS error, the research team used the reported vehicle velocity v_k , from the Oxford system to estimate the future location \hat{p}_{k+1} of the vehicle over a short time step t . This is done using the reported position of the vehicle p_k and current velocity v_k through the equation $\hat{p}_{k+1} = p_k + v_k t$. By comparing \hat{p}_{k+1} and to the actual recorded position p_{k+1} , the estimated GPS error could be determined. However, it should be noted that the measured velocity is in fact a fused estimate from the Oxford unit, which fuses inertial velocity (from the inertial measurement unit) and Doppler velocity, which is reported by the GPS. This approach has a risk of characterizing velocity errors instead of position errors, however the reported velocity is the result of sensor fusion from the inertial sensors and Doppler velocity from the GPS and is therefore expected to be significantly more accurate than the position estimate. The results of this approach are discussed in the recommendations of Chapter 5.

Line Detection Algorithm

To evaluate the use of cameras to inspect road line reflectivity, an algorithm was written to detect the color of road lines using the camera. This algorithm started by extracting the row of pixels directly above the hood of the car in the camera image. This row, due to mounting of the camera, is always pointed on the roadway and the roadway alone when driving on-road. The algorithm then looks across this line of pixels for large deviations in light intensity between neighboring pixels. Large deviations are flagged as potential edges of the road lines. Once the sweep has been completed, the flags are searched for bands of the estimated length of a road line and the color of the original pixels are returned.

Looking for road lines in the LIDAR data proceeds in a similar manner as the camera. However, the row of pixels is replaced by the laser ring that passes just above the hood of the vehicle. This laser ring is then trimmed to 60 degrees to the left and right of directly in front of the vehicle. Then, instead of looking for deviations in light intensity the algorithm looks for large deviations in the intensity of neighboring LIDAR returns. Results of this approach are discussed in Pavement Inspection: Case 1 of Chapter 5.

Cut Grass Analysis

The grass detection algorithm takes a sample of the road in front of the vehicle and uses the height deviation of the LIDAR returns to determine the appearance of a smooth surface. By taking a sliding window of data along a single LIDAR ring, the algorithm classifies the samples as either road or grass based on standard deviation within the window. The length of grass can also be estimated by the maximum difference in vertical height in the grassy areas.

Figure 12 shows a sample image of a data collection location where the grass was recently cut, while Figure 13 shows the same location as viewed by the 64-beam LIDAR.



Figure 12: Camera view of grass detection environment

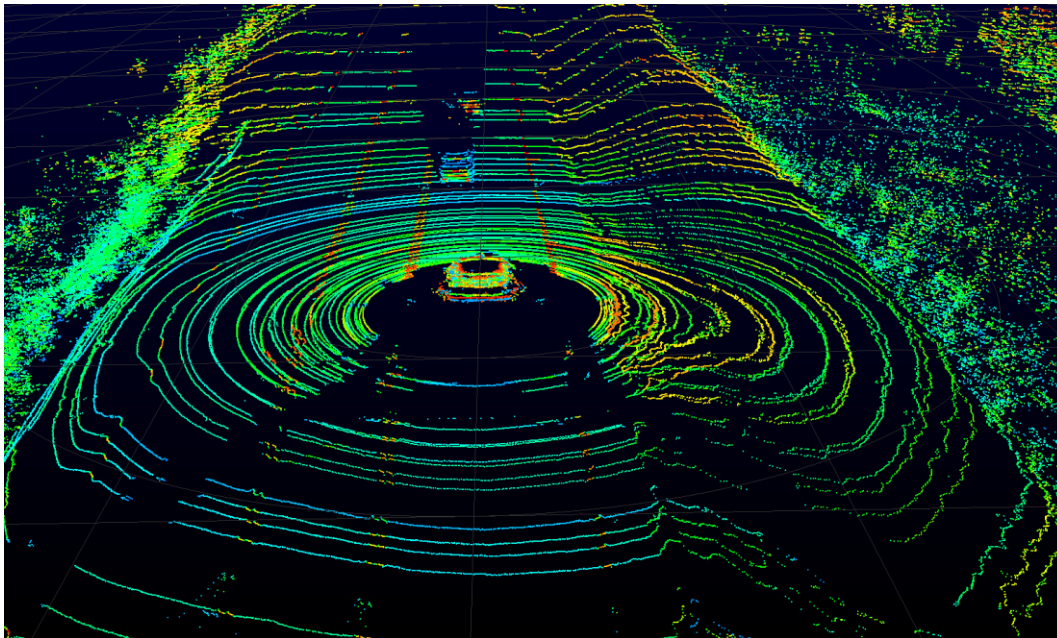


Figure 13: Unprocessed LIDAR returns of grass environment

In order to reduce computational power, a single ring of the unprocessed LIDAR data shown in Figure 13 is used for the line extraction algorithm. The resulting single ring of LIDAR data is shown in Figure 14. However, as seen in Figure 13 the entire set of LIDAR returns from a single laser ring are not on-road and looking at the roadside mowing area. Thus, the algorithm first extracts 50° of the laser ring to either side of directly in front of the vehicle.

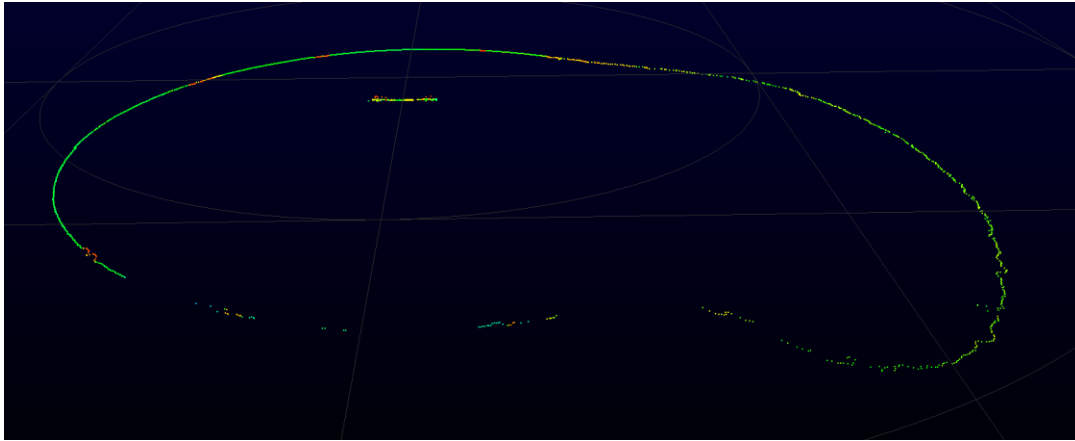


Figure 14: Unprocessed single-laser LIDAR returns

The detection algorithm then takes a 4 consecutive LIDAR returns and computes the standard deviation of the vertical height. If the standard deviation is measured to be below 3 times the a user specified threshold, the LIDAR returns are classified as asphalt. Similarly, if the standard deviation is between 3 and 8 times this threshold the LIDAR returns are classified as cut grass and classified as uncut grass when exceeding 8 times this threshold. The algorithm then moves to the next four samples and classifies these samples in the same manner. The resulting output and the sample windows can be seen in Figure 15.

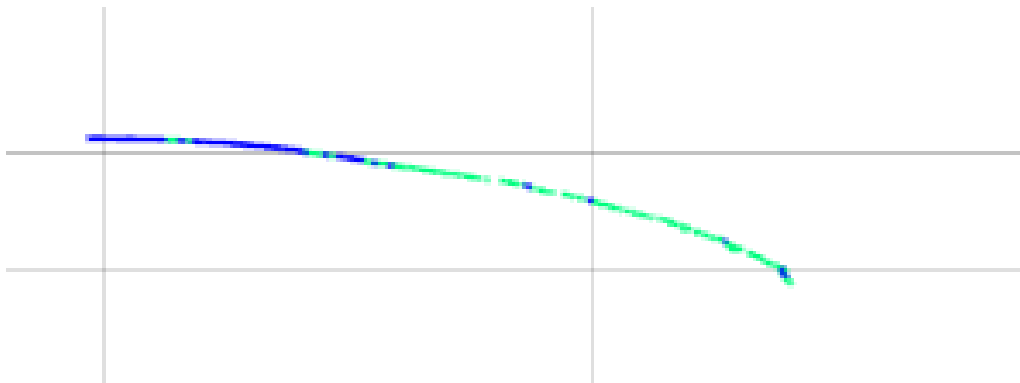


Figure 15: A sample of the LASER ring in the previous figure LIDAR points classified as road (blue) and grass (green)

Communication System Risk Analysis

There are three major organizations that define the standards for automotive electromagnetic compatibility. There are two international organizations called CISPR and ISO and a North American focused organization called SAE. It is common for SAE to develop standards for the North American market, which are then passed to CISPR and ISO for international consideration. When a SAE standard becomes an international standard under CISPR or ISO, the original SAE standard is deprecated.

Since most automotive manufacturers sell vehicles worldwide, they use CISPR and ISO standards to set their internal corporate standards. The major standards that are applicable are shown in the table below.

Table 3: CISPR and ISO Standards applicable to Autonomous Service Vehicles

ISO- 11451	Road vehicles — Vehicle test methods for electrical disturbances from narrowband radiated electromagnetic energy
ISO-11452	Road vehicles — Component test methods for electrical disturbances from narrowband radiated electromagnetic energy
ISO-7637	Road vehicles — Electrical disturbances from conduction and coupling
ISO-10605	Road vehicles — Test methods for electrical disturbances from electrostatic discharge
CISPR 12	Vehicles, boats and internal combustion engines – Radio disturbance characteristics – Limits and methods of measurement for the protection of off-board receivers
CISPR 25	Vehicles, boats and internal combustion engines – Radio disturbance characteristics – Limits and methods of measurement for the protection of on-board receivers

ISO-11451 applies to emissions radiated from the vehicle and is similar to CISPR 12. ISO-11452 applies to external radio signal impinging upon the vehicle and is similar to CISPR25. ISO 7637 is a test standard relating to the possibility of interference being introduced through the vehicle wiring. ISO-10605 covers the concerns of static discharge from humans damaging the electrical components.

The ISO and CISPR standards substantially overlap, differing predominantly in measurement limits and measurement techniques. To simplify the discussion, the following sections focus on the CISPR standards.

CISPR 25 and CISPR 12

The CISPR standards can be divided into two major standards. CISPR 12 focuses on the emissions produced by a vehicle and its sensors. CISPR 12 is geared to prevent the vehicle from interfering with the operation of electronic systems outside of the vehicle. Since this standard focuses on the vehicle’s impact on others this standard is often used in government regulations for vehicle emissions. Governments use CISPR 12 to mandate emission level limits and frequency ranges.

CISPR 25 deals with the effects that external radio disturbances have on the vehicle’s electronics. In general, standards like CISPR 25 are not used in a regulatory manner, rather the vehicle manufacturers work with the component suppliers to determine which standards and which severity levels to apply. The idea is that if the vehicle/component does not perform as

required then the vehicle will be unreliable resulting in unhappy customers and reduced sales.

Electromagnetic compatibility tests are difficult to define. Small differences in the test setup can produce significant variations in the results. In order to assure the measurements are repeatable and verifiable, tests performed in a laboratory under controlled conditions are preferred. But test facilities large enough to accommodate an entire vehicle are expensive and rare. The CISPR 12 standard allows measurements to be performed either at an outdoor test site or in an absorber lined shielded enclosure. The current specifications do not provide a method to correlate the results of the laboratory test to outdoor test measurements. Having the possibility that a vehicle can pass one set of test conditions but not the other may indicate the tests are not accurately measuring the parameters that they are designed to measure.

Standards and Safety

CISPR 25 currently is not subject to governmental regulation. However, with the advent of autonomous vehicles, electromagnetic interference can have a direct impact on safety. Attempting to regulate autonomous vehicle electromagnetic compatibility safety is a difficult task. The ISO11452 and CISPR 25 standards document numerous tests with varying severity levels.

The ISO1145 document describes a Functional Performance Status Classification (FPSC). No specific values for the test signal severity level are defined in the standard. They are to be determined by combined knowledge of the vehicle manufacturer and component supplier. The FPSC begins by defining classes of operation from A to E.

- Class A The device must operate within specifications throughout the entire interference event.
- Class B The device must operate through the transient but it can violate some of its specifications during the interference event and then return to normal operation afterwards.
- Class C One or more of the device functions do not operate during the interference event but normal operation returns afterwards.
- Class D One or more of the device functions do not operate during the interference event but normal operation requires a reset to occur.
- Class E One or more of the device functions do not operate during the interference event but normal operation does not return.

The classes are assigned by an estimate of how safety critical the component is and how well the vehicle can handle failure of this component. For instance, if there are vision, radar, and LIDAR systems performing a similar function, the loss of any one of these systems may not have a significant effect on system safety and may be class C or D. On the other hand, a system that is solely responsible for vehicle throttle or steering would be a class A system.

The vehicle manufacturers then define the test severity levels and the appropriate frequency bands. A chart of the test frequencies and severity for each class is then constructed.

Examples of what these charts might look like are shown below:

Table 4: Example of Test Severity Levels for Incident Field

Test Severity Level	Incident Field V/m
I	10
II	25
III	50
IV	100

Table 5: Example of Frequency Bands

Test Levels	Frequency Range, F
F1	<100kHz
F2	100kHz < F < 10MHz
F3	10MHz < F < 500MHz
F4	500MHz < F < 2GHz

Table 6: Example of Field of View Severity Levels Matched to Frequency Bands

Test	Class A	Class B	Class C	Class D	Class E
F1	II	II	I		
F2	II	II	I		
F3	III	II	II	I	
F4	II	I			

While allowing the vehicle and component manufacturers set the standards that their products must meet may not seem like appropriate oversight, it is unlikely that any government organization has more knowledge of the products and their weaknesses than the manufacturers. Electromagnetic compatibility test severity levels and frequency bands should be determined by leveraging the expertise of the component and vehicle manufacturers. Safety of the vehicle after sale can be assured through existing mechanisms that document vehicle safety failures such as the Safercar program run by the National Highway Traffic Safety Administration.

Chapter 5: Recommendations

The recommendations made by the research team focus on two autonomous service vehicle tasks: roadside mowing and pavement inspection. For each task, a set of risk cases were identified based on the completed analysis. These risk cases are shown below, along with evidence of the risk associated with the case and a recommendation for mitigating the risk associated with the individual case. The research team also considered modes of operation when making communication recommendations for each service task.

Mowing Risk Cases

Case 1: GPS accuracy in open areas

Evidence: As found in the literature, a standalone GPS system has an expected accuracy of 1 meter or more. Using an INS in conjunction with GPS, the precision and repeatability can be greatly increased, but the absolute accuracy can remain the same when moving at slow speeds. This investigation found that when operating in clear line of sight to the sky the GPS precision algorithm presented in Chapter 4 showed an average GPS error of 0.54cm, median error of 0.13cm and a maximum reported error of 9.5cm.

Recommendation: In an area without ground coverings, such as an open field, a GPS/INS system or GPS with correction services can give sufficient accuracy to ensure the system does not enter onto a roadway. To ensure proper coverage for mowing, it is recommended that the system plan for overlap in mowing swath of at least 10cm. Furthermore the path the mower takes should remain at least 10 cm from the road's edge to prevent road incursion. In the event of GPS dropout or loss of corrections, the vehicle must come to an immediate stop or have a human operator take control of the platform to prevent road incursion.

Case 2: Areas with heavy tree cover and tall buildings degrade even corrected GPS quality

Evidence: Unlike open areas, tree cover and tall buildings can cause significant errors in the position estimate of a GPS/INS system. This was shown in the data collected on Old Dixie Highway in Ormond Beach, Florida where the tree canopy extends to cover much of the roadway, as shown in Figure 16, and when collecting data in close proximity to tall buildings in downtown Orlando, FL. While operating under tree cover the team found a relatively low mean error of 1.09 cm, and a median error of 1.1mm. However, the errors from the fused GPS/INS position estimate were observed as high as 4.8 m, with 0.2% of cases exceeding 0.5m of error and 0.06% of cases exceeding 1m of error. Operating in proximity to tall buildings showed errors as high as 2.92m, with 0.2% of cases exceeding 0.5m of error and 0.11% of cases exceeding 1m of error. This error is not just predicted by the algorithm used here, but can also be seen in the GPS/INS data, as illustrated in Figure 17. While rare, these instances of reduced accuracy were observed to last for up to a 2 second period. It should also be noted that the project vehicle had to operate on paved surfaces or in closer proximity to the roadway for safety reasons. Thus, an all-

terrain mower may get close to trees or buildings and experience more significant errors than reported here.



Figure 16: Tree Cover on Old Dixie Highway in Ormond Beach, FL.

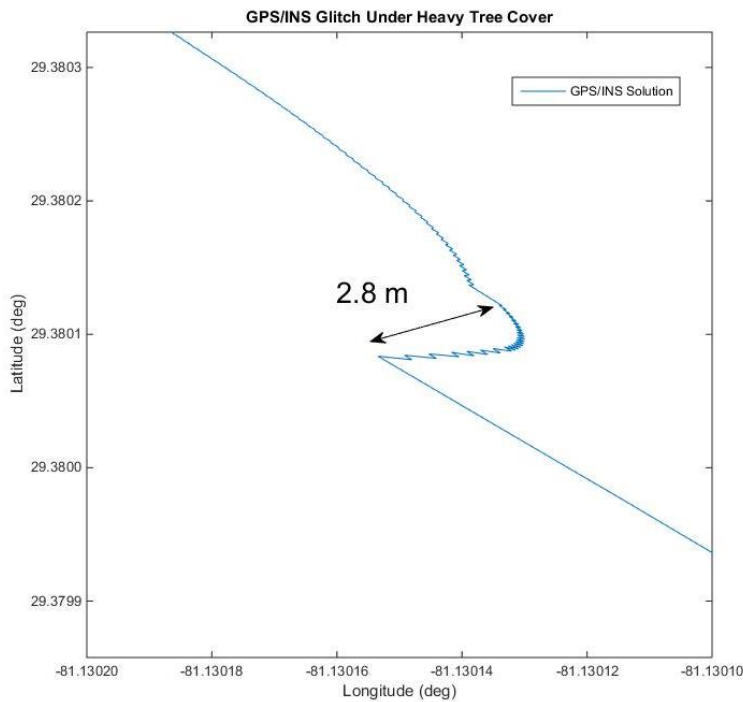


Figure 17: A snapshot of the GPS path during traversal on Old Dixie Highway in Ormond Beach, FL.

Recommendation: For mowing operations using purely GPS in heavy tree cover, a large overlap in the swaths or multiple mowing passes would be needed to compensate for the short duration inaccuracy of the GPS. This could make the operation highly inefficient. However, road incursion is a bigger concern and could occur even with the short durations of GPS error observed in this study. Thus, it is recommended that for all mowing operations, but especially

under heavy tree cover, a sensor is used to detect the grass that needs to be mowed rather than relying solely on the GPS to follow a pre-planned route. This adds redundancy to ensure the platform is operating in the desired area.

Case 3: Resolution of LIDAR measurement needed to detect grass quality

Evidence: Figure 18 shows a sample result of the previously discussed algorithm for detecting cut grass using the LIDAR. This figure plots the ground surface, and colorizes the LIDAR returns based on whether the terrain is classified as asphalt (blue), cut grass (Green), or uncut grass (yellow). This approach was applied over the course of a five minute data collection, with a consistent ability to distinguish asphalt from grass, with cut grass from uncut grass still under evaluation. In this area, the roadway extends from roughly $y = 0m$ to $y = 1.5m$, the cut grass region then extends to $y = 4m$, and the rest of the grounds are uncut. While the algorithm used here is fairly basic in nature, and does sometimes confuse asphalt and cut grass, it clearly illustrates the ability of a LIDAR to detect areas where grass is yet to be cut. Knowing where grass needs to be cut can improve mowing quality and be used as a supplement for preventing road incursion.

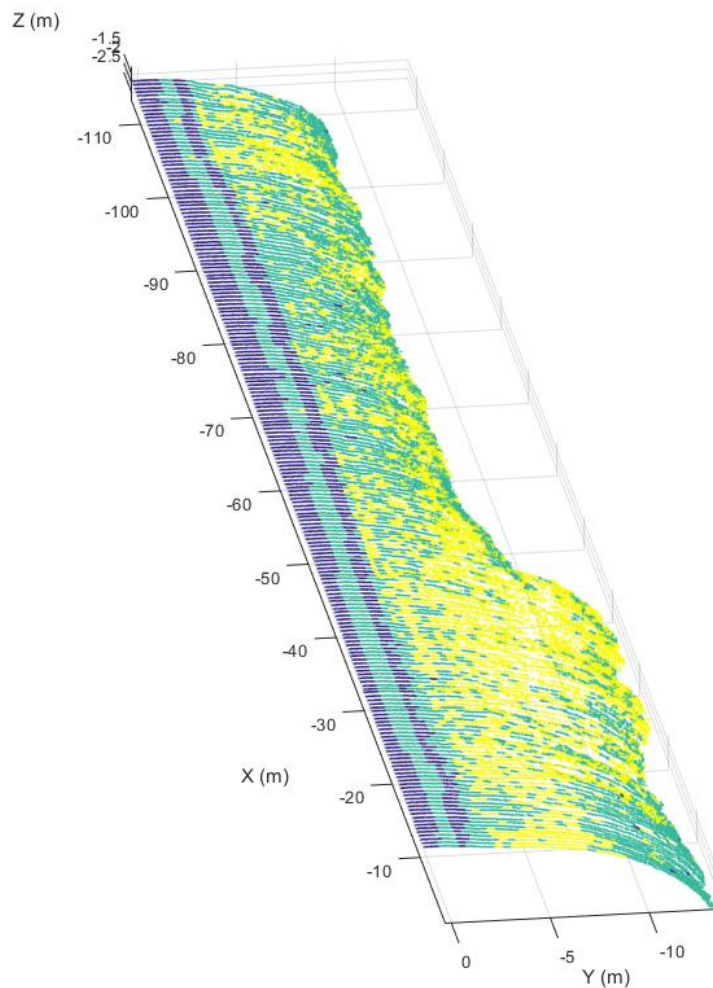


Figure 18: Sample result of Asphalt (blue), Cut Grass (green) and Uncut Grass (yellow) detection.

Recommendation: Based on findings from the cut grass identification algorithm, a single laser ring at a 0.46° resolution or finer and a 5Hz spin rate is able to distinguish cut grass from uncut grass and road surfaces when the LIDAR is mounted 2m above ground. This corresponds to a minimum resolution of approximately 5cm between LIDAR returns on the ground.

Case 4: Rough ground will cause high vibrations and potentially cause data dropouts

Evidence: While collecting data on gravel and dirt roads, the vehicle experienced abnormally high vibrations. This is shown in Figure 19, where vertical acceleration is shown to be consistently below 2 m/s^2 on roadways, and frequently above this threshold on dirt roads. These vibrations were found to create a loss of data during playback (see Figure 20). While the team used a computer with a solid state drive during most of the data collections, this particular run was conducted using a back-up computer that used a traditional hard-disk drive to see if the platform observed this data loss. Data loss could potentially occur on autonomous systems due to communication dropouts as well, which unlike data storage, can affect real-time processing.

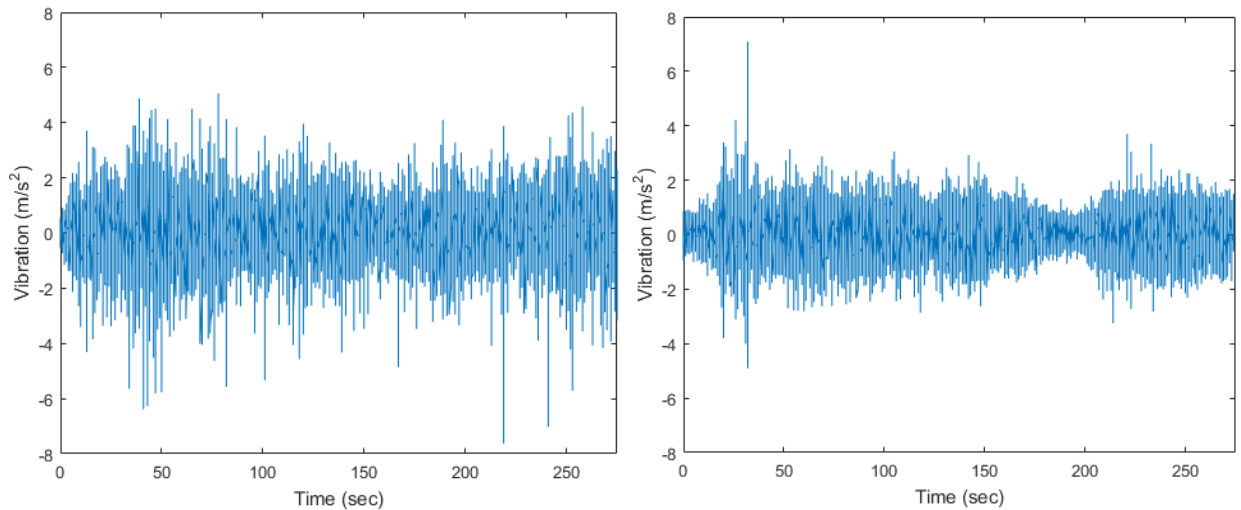


Figure 19: Samples of measured vertical acceleration of the vehicle on a dirt road (left) and on a paved roadway (right).



Figure 20: Data loss shown in the LIDAR playback

Recommendations: There are two simple solutions to solving the vibration problem. The first solution would be to utilize a solid-state disk for recording data, as it is much more resistant to vibration than a traditional hard-disk drive. The second solution would be to add a software buffer on the data, so that incoming data can be stored in a queue in case the hard drive loses performance over a bump. However, the software solution begins to break down in more consistent vibration environments, and is not as resilient as a solid-state hardware replacement solution. To avoid problems associated with communication dropouts, autonomous service vehicles should use high sampling rates (5 Hz or greater) and have their connectors routinely inspected for failures.

Case 5: Effectiveness of LIDAR at recognizing construction objects

Evidence: The images displayed in Figure 21 and Figure 22 show that the LIDAR has no trouble detecting construction barrels due to the reflective striping. The high intensity returns and density of returns seen here allows for classification of these objects, which indicate a construction zone.

The autonomous vehicle can then adjust course or speed based on the location of the barricades. However, while smaller LIDAR sensors can still detect the barricades as an obstacle, a multi-beam LIDAR would be required to consistently and accurately classify the barrels using the reflective striping and shape of the object. Similarly if a mower is operating while these barrels are in the grass, treating them as objects enables the platform to maneuver around them off-road.



Figure 21: Camera view of construction zone, including concrete barriers and construction barrels.

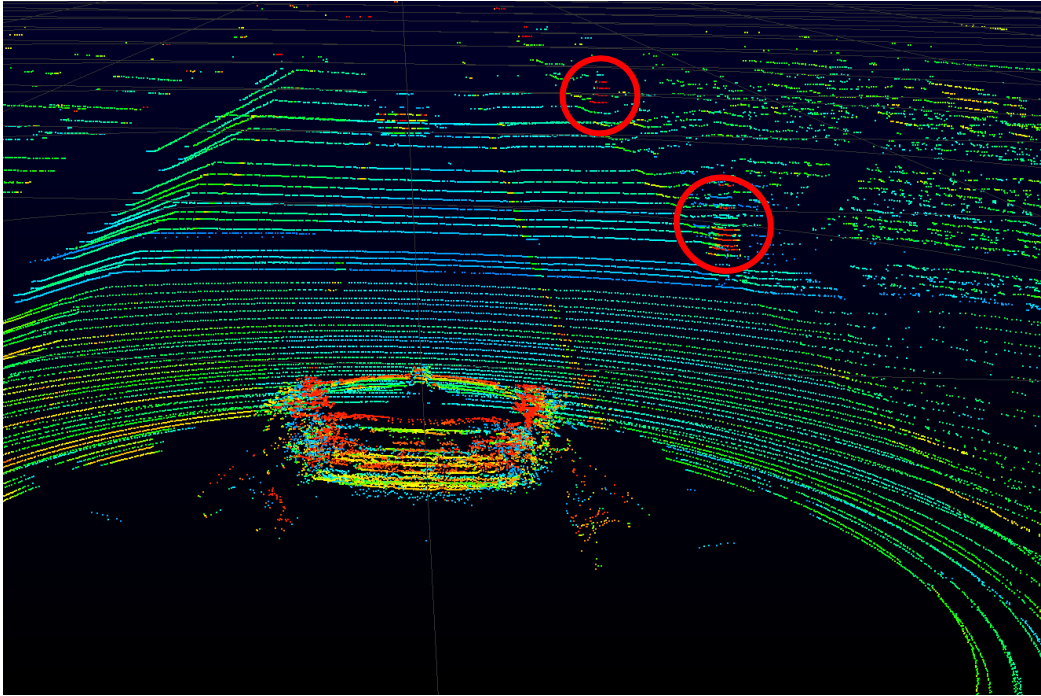


Figure 22: LIDAR returns in a construction zone. High reflectivity objects make more apparent markers of construction areas.

Recommendation: To consistently recognize reflective construction barrels and cones, it is necessary to use a LIDAR with at least 5 laser beams intersecting the object at the desired recognition distance. If recognition is not needed and only avoidance, a single-beam LIDAR can be used to detect the presence of construction barrels and cones.

Case 6: Operating near cliffs or areas with large drop-offs

Evidence: Cliffs and drop-offs appear as empty areas in data recordings.

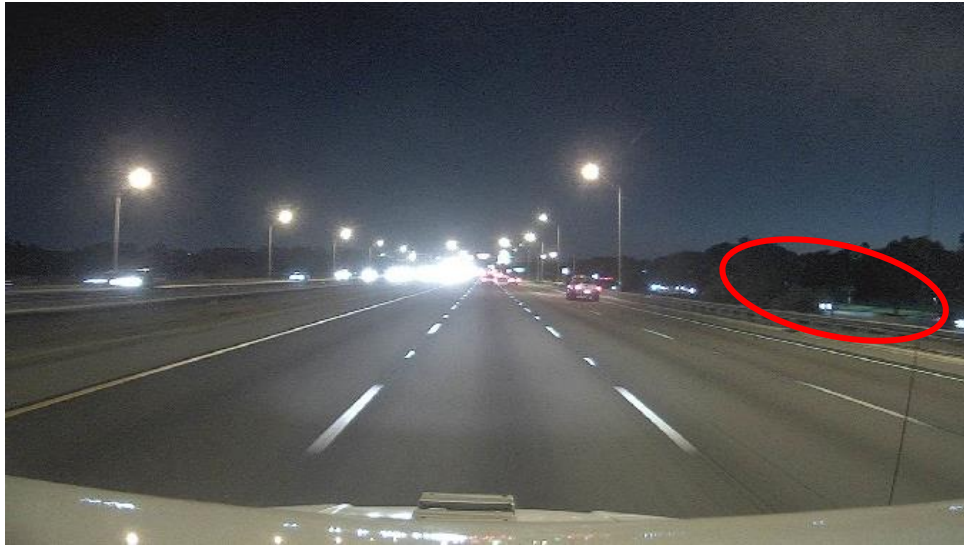


Figure 23: Camera Image when crossing over a bridge.

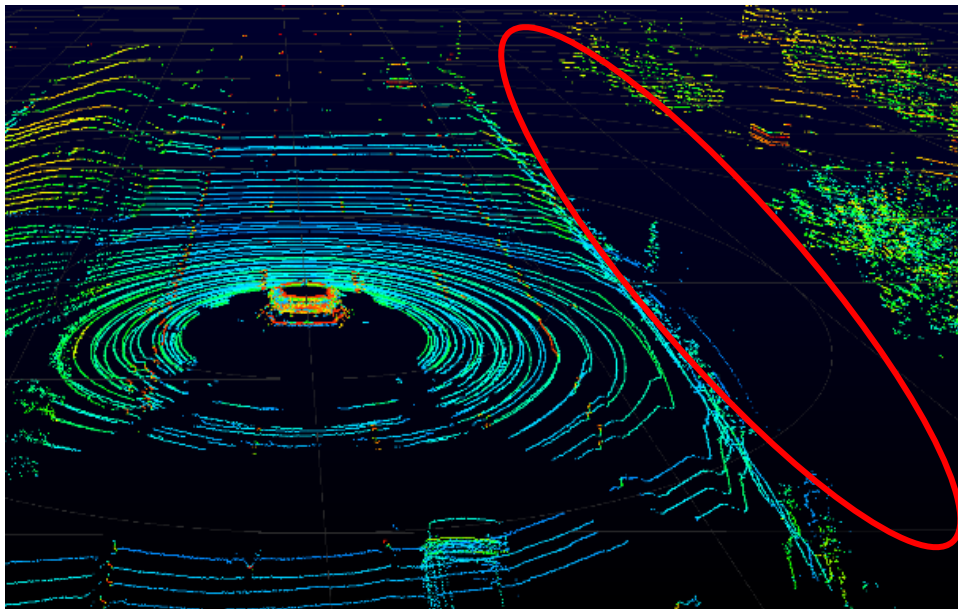


Figure 24: LIDAR data recorded when crossing over a bridge.

Recommendation: As with manned operations, mowing near a cliff or drop-off should be considered an unsafe condition for an autonomous mower. A geofence can be used to keep the

mower sufficiently far from these areas (but this is subject to GPS accuracy as in Roadside Mowing Case 1 and Case 2). Additionally, areas with few LIDAR returns can be flagged as not traversable and avoided by the vehicle. It is recommended that grass close to such drop-offs be cut in the same manner as they are currently cut with manned operations.

Case 7: Detection of obstructions and obstacles

Evidence: Figure 25 shows a large vehicle off of the side of the road and how it is seen by both the LIDAR and radar sensors. Looking closely at the LIDAR image shows that the man fixing the vehicle is still visible. However, the radar is only able to see the outline of the large truck as an obstacle. This is due to the human body being a poor reflector of radar frequencies. Other materials are similarly difficult to detect by the radar, as seen in Figure 26 where the plastic tarp barricade is detected by the LIDAR and not the radar.

Recommendation: The LIDAR is less sensitive to material type than a radar, and is more accurate at gauging distance than camera solutions. However, radar provides velocity estimates and is effective at detecting large vehicles. Similarly a camera is useful at providing information such as color and shape that can be useful for identification of perceived objects. Thus, it is recommended to use LIDAR for general obstacle avoidance, and to supplement this information with a radar when velocity information is needed and a camera when object identification is required for platform decision making.

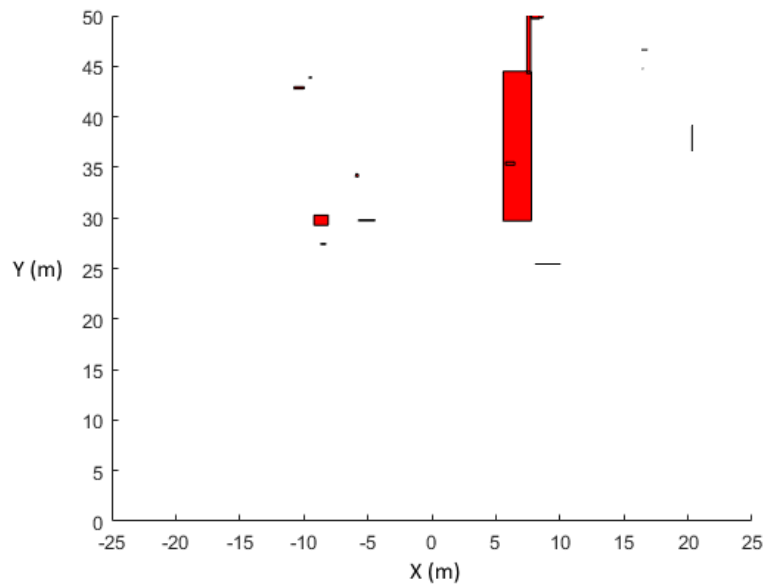


Figure 25: Vehicle obstruction as viewed by the camera and LIDAR. The man working on the truck is highlighted with a red circle in the camera image and LIDAR plot. The area where the man is working is highlighted with a red circle on the radar plot. The two green dots above the red circle in the radar plot are from the truck and trailer.

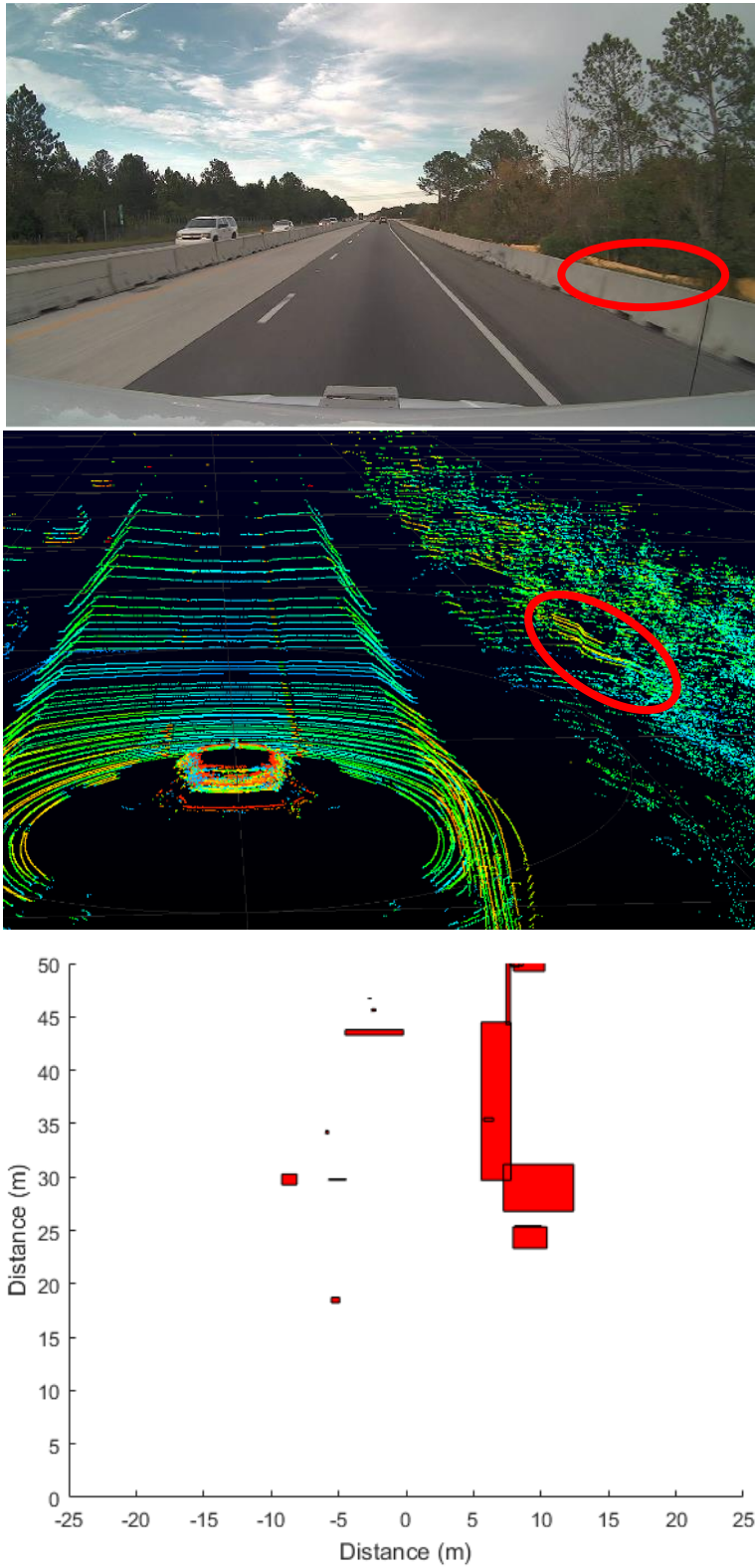


Figure 26: Plastic mowing obstruction as viewed by the camera, LIDAR and radar.

Case 8: Mowing at night and in low-light scenarios

Evidence: At night, the use of cameras to determine areas that have been mowed is subject to the quality and strength of local area lights or onboard lighting. Most areas will not have local lighting and bright lights on the mower itself could create a safety hazard for nearby drivers. However, as shown in Figure 27, LIDAR returns are nearly identical in both daytime and nighttime conditions. Thus a camera will have difficulty perceiving areas as being cut grass or uncut grass without significant onboard lighting, while this is not when using LIDAR to detect the terrain.

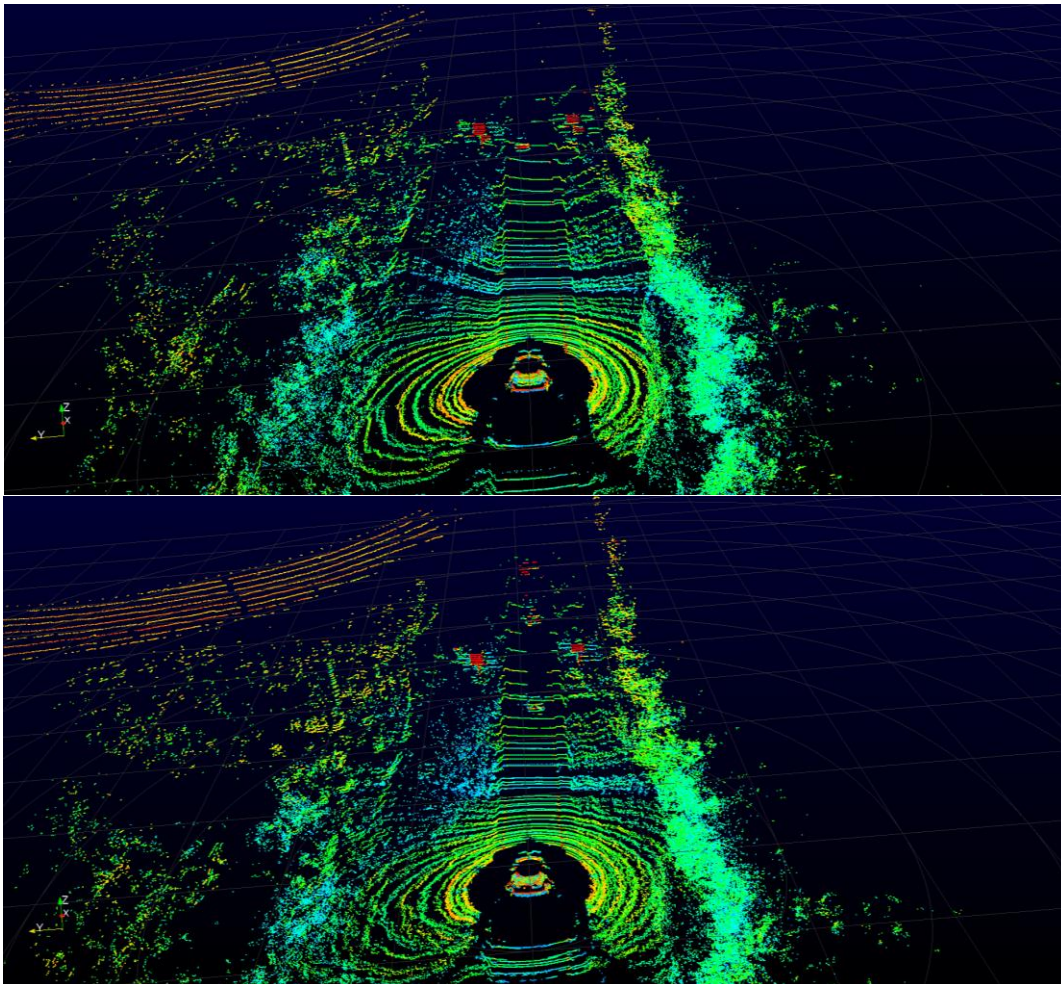


Figure 27: LIDAR data collected during daytime (top) and at night (bottom) on the roadway.

Recommendation: As LIDAR is not affected by ambient lighting conditions, it is recommended to use LIDAR to detect areas of cut and uncut grass. Furthermore, this means that mowing operations can occur at night. However, mowing operations at night have potential safety risks to unaware manned vehicles operating on adjacent roadways. Thus the mower needs to be clearly visible while not impeding the visibility of these drivers. Further studies should look into standard operating procedures for nighttime mowing since these operations are not currently conducted at night.

Mowing Operation Scenarios

Scenario: Line of Sight Operation

Scenario Description: In this scenario the service vehicle is accompanied by a remote operator who maintains line of sight proximity with the vehicle. The operator has the ability to directly control the vehicle through a remote command and control link. The operator can also command the vehicle to begin, pause, stop, and modify its autonomous behavior.

Communication Recommendation: In this operating scenario no long distance radio data links are required. Monitoring, command, and control data can be sent over short, and mid-range data links in the ISM bands. The command and control links can be low data rate (< 115200 baud) robust links (spread spectrum, frequency hopping) to mitigate any potential interference and increase range. The control link must be properly secured to prevent unwanted intrusion or loss of control. Monitoring links should be higher data rate links capable of streaming video and/or sensor data (1MB/s). This can be achieved with one radio link or using multiple radio links.

Scenario: Command Center Operation

Scenario Description: In this scenario the service vehicle is left on site with no operator within line of sight. Monitoring, command, and control are performed at a remote "Command Center". The command center operator has the ability to directly control the vehicle through tele-operation. Tele-operation would require a minimum of 360 degree field of view camera video transmitted to the operator. The operator can also command the vehicle to begin, pause, stop, and modify its autonomous behavior.

Communication Recommendation: This operating scenario requires one or more long distance data links. The command and control links can be low data rate links (<115200 baud) to increase range. The control link must be properly secured to prevent unwanted intrusion or loss of control. The link used for monitoring should be high data rate (1-2MB/s) and for this low speed operation, have an inherent latency of 100msecs or less. The control link should also have a heartbeat signal that causes the vehicle to enter a safe mode if the link drops or becomes intermittent.

Command Center Monitoring

Scenario Description: In this scenario the service vehicle is left on site with no operator within line of sight. Monitoring, command, and control are performed at a remote "Command Center". In this scenario there operator does not have the ability to directly drive the vehicle remotely. The command center operator does have the ability to monitor the vehicle systems. The operator can also command the vehicle to begin, pause, stop, and modify its autonomous behavior.

Communication Recommendation: This operating scenario requires one or more long distance data links. The command and control links are again only required to be low data rate links (<115200 baud), with a latency of 100 msec. The control link must be properly secured to

prevent unwanted intrusion or loss of control. The monitoring links can either be a high data rate link that allows viewing of live video and sensor data (1-2 MB/s) for diagnostic purposes (e.g. verifying reported task completion and obstructions) or it can be a low data rate link (<115200 baud) that enables the operator to view only vital system states (fuel levels, faults, progress). The data link could tolerate latency delays of up to 500msecs as the vehicle should be able to operate safely without any low-level platform control. The control link should also have a heartbeat signal that causes the vehicle to enter a safe mode if the link drops or becomes intermittent. The data links may also be short range links to an internet access point and then be routed anywhere in the world.

Pavement Inspection Risk Cases

Case 1: Detection of road lines and characterizing line reflectivity

Evidence: Although lines can be reliably detected due to a consistent contrast between the pavement and roadways, the observed color from camera imagery varies significantly with shadows, weather conditions, and time of day. This is shown in Figure 28, where the color of the detect line is clearly changing as more camera frames are acquired. It should be noted that there were gaps in the road lines in frames 80-85 and frames 115-120. Tests also showed that concrete curbs can give similar camera intensities to road lines, which could confuse line identification.

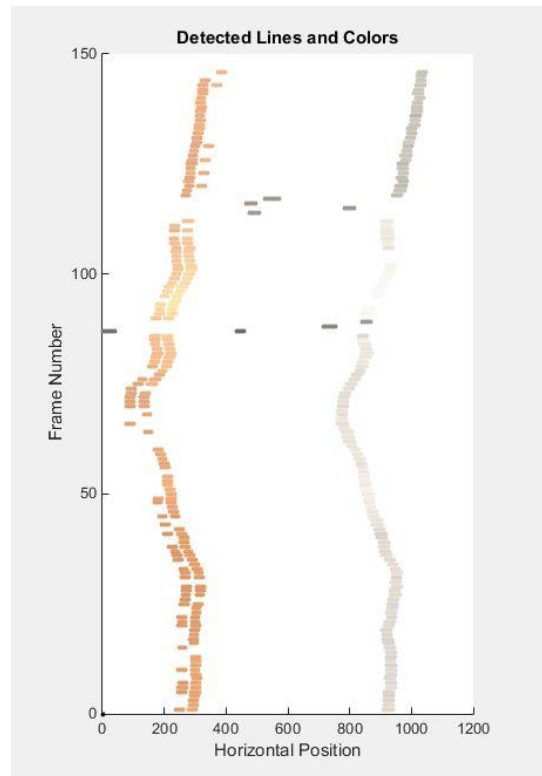


Figure 28: Line Detection results for Tomoka Farms Rd, in Port Orange, FL. The lines here show the detected color of the road line as viewed by the onboard camera and the horizontal position within the camera frame.

LIDAR samples were examined to determine if intensity of LIDAR returns could be used to determine line reflectivity. A summary of this investigation is given in Table 7. Note that, LIDAR intensities are reported as a value from 0-255, with 255 being the maximum reflectivity.

Table 7: Summary of LIDAR intensity analysis for line reflectivity

Test Location	Intensity Values			Sample Size
	Mean	Median	Std Dev	
I-95 (Lines)	136.38	32.72	121.50	221
I-95 (Roadway)	59.38	12.83	55.00	3976.00
Williamson (Lines)	175.74	35.40	188	182
Williamson (Roadway)	43.51	8.73	43	3195
Willow run (Lines)	150.00	139.00	42.03	6
Willow run (Roadway)	69.36	65.00	18.61	1916

This inspection showed that the mean LIDAR intensity of road lines in these environments are consistently in the range of 135-180, while the roadway gives a mean intensity in the range of 40-70. Similarly, the median intensity of the road lines is consistently higher than that of the pavement. This means using the LIDAR should be effective at distinguishing the lines from the paved surface. The LIDAR may also be able to distinguish line quality, as it is seen here that the road lines that have were striped only a few days before data collect (the Willow run Road trial) yielded consistently higher LIDAR intensities.

It should be noted, that the high standard deviation in road lines for I-95 and Williamson roads are due to the use of retro reflectors on these roadways. When excluding these samples, which are a small number of the total line samples, the LIDAR intensities are fairly consistent (as evidenced by the median intensity), and have less deviation than the lines seen in camera imagery. This is due to the fact that the LIDAR intensity is referenced to a known lighting source while the camera uses the uncontrolled lighting of the sun and sporadic man-made lighting.

Recommendation: Cameras can be used to detect the existence and type of road markings, but are unreliable in determining road marking quality. It is recommended that a single or multi-beam LIDAR be used to detect the quality of road lines for potential striping. It should be noted however, that a LIDAR will measure reflectivity in a different band (typically 905nm) than visible light. Thus, LIDAR inspection is only practical if the paint is known to have a similar reflectivity in both bands.

Case 2: Detection of potholes

Evidence: The image below shows a stretch of roadway with several potholes in the dirt road. The LIDAR returns clearly show these deviations. However, this is significantly harder to see in the camera imagery.



Figure 29: Sample pothole data on local roadways in Volusia County

Recommendation: Based on collected data, detecting potholes of a specific depth requires a LIDAR with distance accuracy less than half the depth of the pothole to be detected. Angular resolutions of 0.46 degrees and finer on the LIDAR sweep were found to effectively find potholes with a roof-mounted LIDAR. Lower angular resolution systems can potentially be used if the LIDAR is mounted closer to the ground. Also, the speed at which the vehicle moves can result in significant gaps in ground coverage for single beam LIDAR systems. Thus, a multi-beam LIDAR system is recommended and the speed of the vehicle must be slowed based on the angle between laser rings and the scan rate to ensure potholes are seen. A small vertical angular resolution is highly recommended to enable data collection at higher vehicle speeds. It is further recommended that mapping techniques be pursued to intelligently combine data from multiple laser scans into a more accurate pothole representation.

Case 3: The effect of wet roads on pavement inspection and autonomous operation

Evidence: Testing indicated that road lines are difficult to detect reliably in wet weather conditions. Camera imagery degrades due to lens obstruction, reflections, and specular reflections. It was also found that the total number of LIDAR returns is reduced by 40-60%, with a majority of the lost returns coming from the pavement surface. Furthermore, the difference between LIDAR intensity on road lines and pavement noted in Pavement Inspection: Case 1, is virtually non-existent. This can be seen in Figure 31 where water on the roads has reduced all road intensities to a low intensity level (indicated by blue coloration), and few returns are even observed beyond a car length in front of the vehicle. These issues were less severe when raised pavement markers are used on the roadway, as the markers were highly visible to the LIDAR and camera. However, infrastructure changes were outside the scope of this investigation.

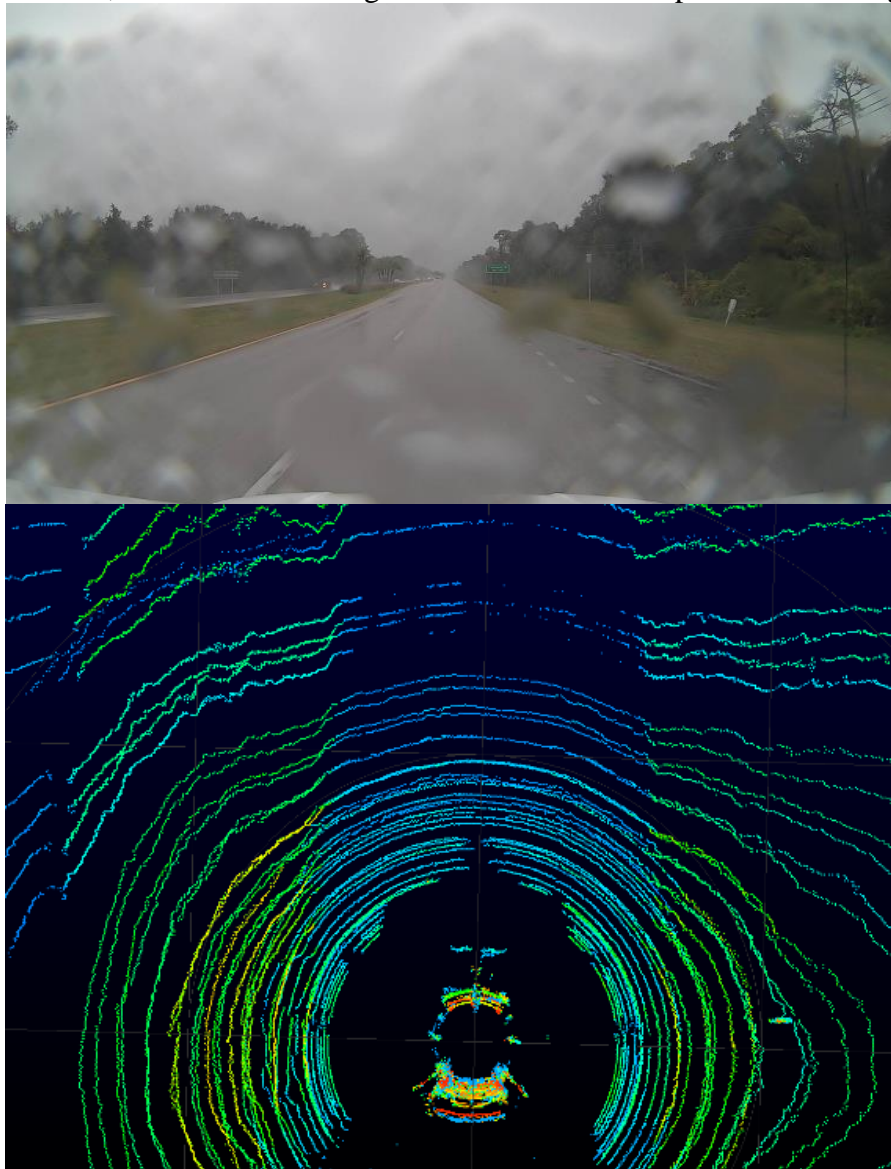


Figure 30: Camera and LIDAR view of road lines in rainy conditions. There is no standing water on the roadway.

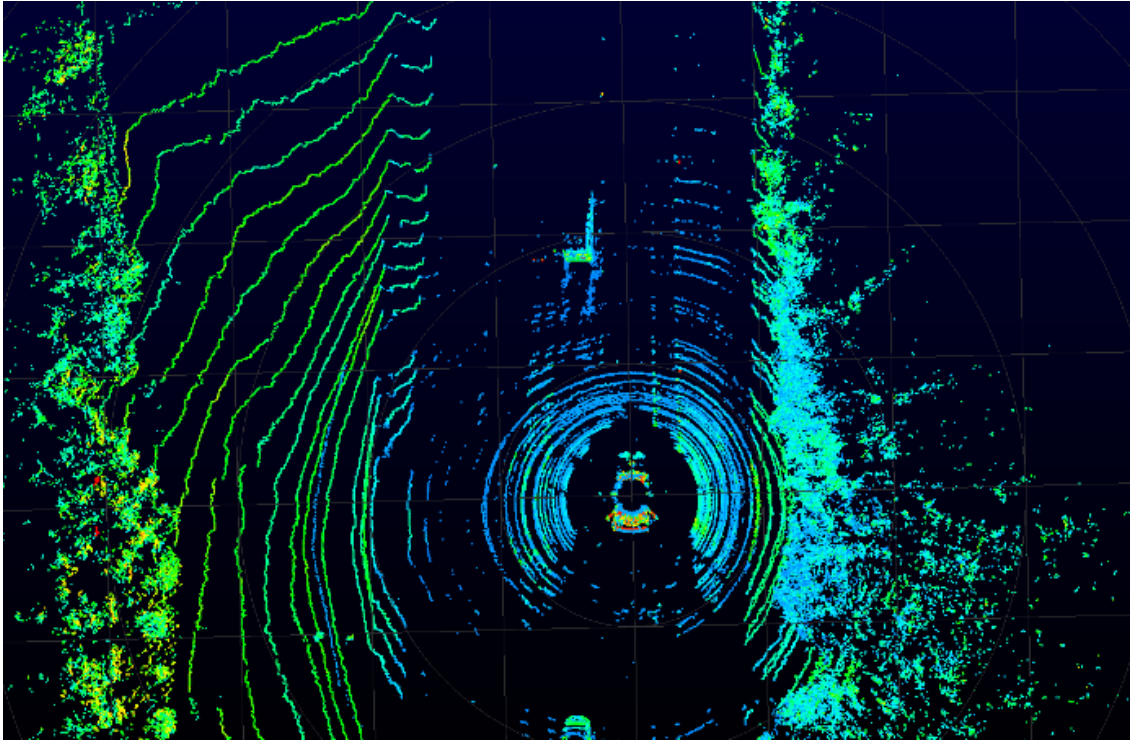


Figure 31: LIDAR view of a road covered in a thin layer of water (less than 1 cm) due to heavy rain

Recommendation: On a moderately wet roadway, a camera can still detect the road lines as long as there is no precipitation, although splash from other vehicles can obscure the camera feed. Alternatively, the camera can be placed inside the vehicle if it is a passenger vehicle with wipers. In light precipitation, the LIDAR can still be used to see obstacles and potholes (without standing water), but it is not able to detect lines reliably. In moderate to heavy rain, it is recommended to avoid service operations altogether. For inspection of lines and roadways, it is recommended to only operate in dry conditions.

Case 4: Operating under bridges

Evidence: Figure 32 shows radar data collected when traversing under a walkway. This figure shows that the radar identifies multiple objects from 15-20m in front of the vehicle, which are actually returns from the pedestrian walkway. The false objects would make the vehicle think there is an obstruction in the road. Overpasses, bridges, and metal poles with traffic lights over the roadway can also give false positive radar returns of this nature. Figure 33 shows that the LIDAR has sufficient vertical resolution to differentiate between points above the roadway and see there is not an obstruction ahead.

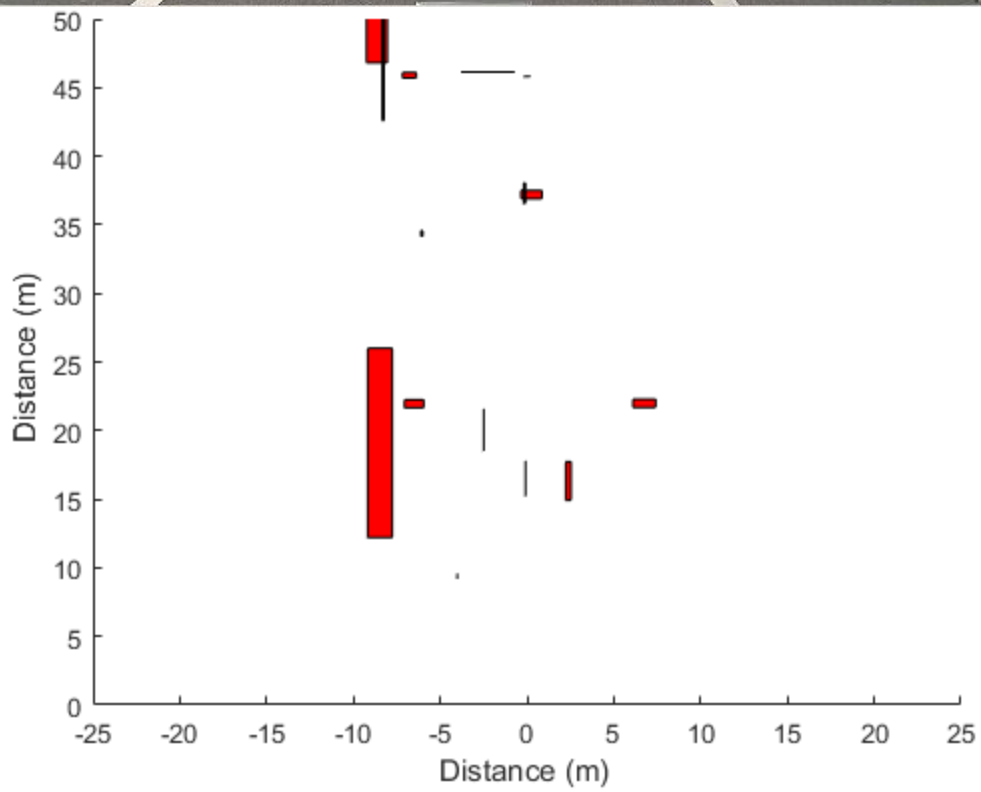


Figure 32: Pedestrian walkway as viewed by the camera and RADAR

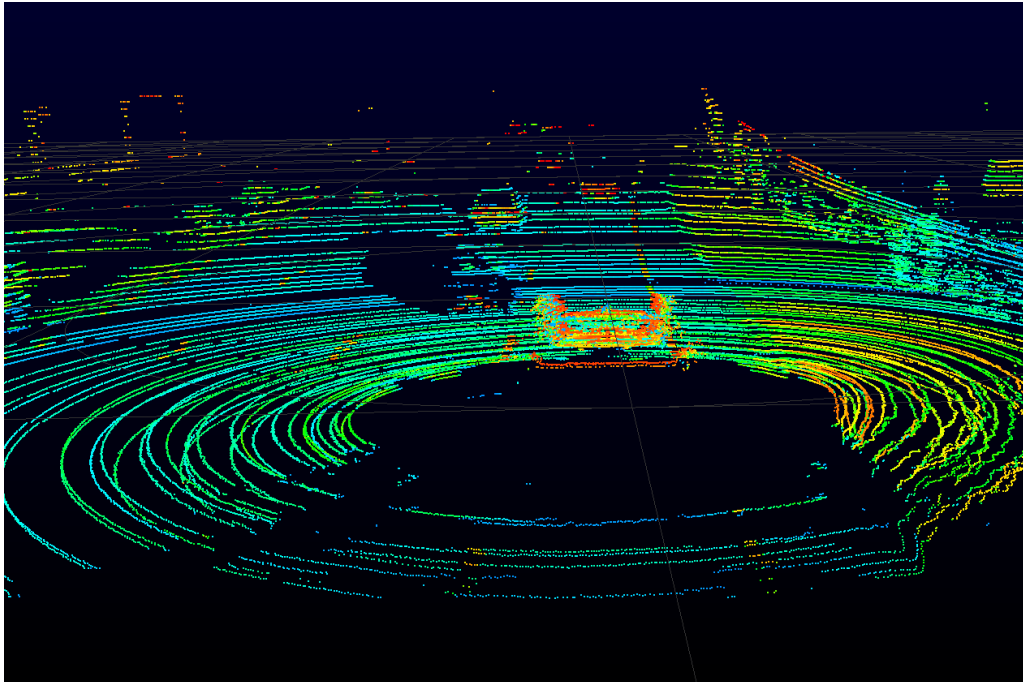


Figure 33: LIDAR view of the pedestrian walkway scene. The walkway is not visible since the LIDAR beams point up at a maximum of 2 degrees with respect to the horizontal plane.

Recommendation: While a small vertical field of view could mitigate this issue, this strategy will likely be insufficient when traversing slopes, which can be particularly severe for off-road vehicles. Thus, it is recommended that service vehicles use a multi-beam LIDAR and inertial system in coordination with a radar sensor to estimate the ground plane in the operating area and the current attitude of the vehicle. The vehicle can then determine if the objects detected by the radar will cause a collision in three dimensional space instead of using two dimensional collision detection strategies.

Pavement Inspection Operation Scenarios

Scenario: Manned Data Recording

Scenario Description: In this scenario the service vehicle is driven exclusively by an operator. The sensor suite used for inspection can either be automated or controlled by the operator. The operator has the ability to start, pause, and stop data recording and processing by the sensor suite.

Communication Recommendation: This scenario requires no communications with the vehicle. The operator(s) may have a radio handset.

Scenario: Automated Data Recording

Scenario Description: In this scenario the service vehicle is an autonomous vehicle that has the necessary sensor suite for inspection mounted to the vehicle. Data collection occurs onboard the vehicle and processing can optionally be conducted onboard. The platform is manned by an

operator who has the ability to take control of the vehicle, and has minimal interaction with the sensor platform. The sensor platform will notify the operator of routes it is traveling.

Communication Recommendation: This scenario requires no communications with the vehicle. The operator may have a radio handset.

Scenario: Control Center Monitoring

Scenario Description: In this scenario the service vehicle is an autonomous vehicle that has the necessary sensor suite for inspection mounted to the vehicle. Data collection occurs onboard the vehicle and processing can optionally be conducted onboard. In this case, the platform is unmanned. Remote monitoring is performed at a "Command Center". The command center operator has the ability to monitor vehicle health (fuel, faults, progress, etc.) and possibly live sensor data. The command center operator can instruct the vehicle to stop operations safely, stop operations immediately, return to a home location, or modify its route.

Communication Recommendation: This scenario can be achieved using a low data rate (<115200 baud) communication link if only health monitoring and commands are required. If live sensor data is required, a higher data rate link (1-2MB/s) is required. The communication link must be properly secured to prevent unwanted intrusion or loss of control. There should also be a heartbeat on the data link that instructs the service vehicle to safely stop (such as on the shoulder), or return to the command center for diagnostics if communications are lost or intermittent.

Chapter 6: Conclusions

The research team presents recommendations for sensor selection and use to ensure safe and efficient operation of autonomous service vehicles conducting roadside mowing and pavement inspection. Such recommendations include avoiding the use of radar when passing under bridges, avoiding pavement inspections in the rain and the use of sensor fusion to mitigate GPS error. Each of the recommendations are supported with empirical evidence recorded using a sensor payload representative of autonomous service vehicles. Automated data inspection also indicates that LIDAR sensors are effective at inspecting line reflectivity and determining areas with cut and uncut grass. This study also recommends bandwidth specifications for radio links based on modes of operation for pavement inspection and roadside mowing operations.

The presented list of recommendations is meant as a starting point for generating a sensing payload and autonomy algorithms to conduct these operations. The research team believes pilot studies are needed to determine additional requirements for operation and to generate standard operating procedures for autonomous service vehicles. It may also be possible to make minor changes to the transportation infrastructure in order to increase sensing reliability. Such changes could include the use of construction markers that are highly reflective to near-IR LIDAR systems and the increased use of raised pavement markers.

References

- [1] J. L. Jones, "Autonomous Vehicle Report," Florida Highway Safety and Motor Vehicles, Tallahassee, FL, Report #13-008, 2014.
- [2] G. L. Harrison, "Economic Impact of Ecosystem Services Provided by Ecologically Sustainable Roadside Right of Way Vegetation Management Practices," Florida Department of Transportation, Tallahassee, FL, 2014.
- [3] National Work Zone Safety Information Clearinghouse, (2013). Fatalities in Motor Vehicle Traffic Crashes by State and Work Zone [Online]. Available: <http://www.workzonesafety.org/crash-information/workzone-fatalities/motor-vehicle-traffic-crashes-2013/>.
- [4] Program and Resource Plan, (April 2015). Florida Department of Transportation [Online]. Available: <http://www.dot.state.fl.us/OWPB/pr/ProgramAndResourcePlanDocument.pdf>.
- [5] Road vehicles – Component test methods for electrical disturbances from narrowband radiated electromagnetic energy, ISO 1452, 2015.
- [6] Limits and methods of measurement of radio disturbance characteristics of components and modules for the protection of receivers used on board vehicles, CISPR 25, 2002.
- [7] Electromagnetic Compatibility Measurement Procedures and Limits for Components of Vehicles, Boats (up to 15m), and Machines (Except Aircraft) (16.6 Hz to 18 GHz), SAE J1113, 2013.
- [8] P.Vähä, T. Heikkilä, P. Kilpeläinen, M. Järviluoma, E. Gambaob, "Extending automation of building construction – Survey on potential sensor technologies and robotic applications," *Automation in Construction*, vol. 36, no. 1, pp. 168-178, December 2013.